



### 저작자표시-비영리-변경금지 2.0 대한민국

이용자는 아래의 조건을 따르는 경우에 한하여 자유롭게

- 이 저작물을 복제, 배포, 전송, 전시, 공연 및 방송할 수 있습니다.

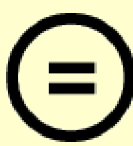
다음과 같은 조건을 따라야 합니다:



저작자표시. 귀하는 원 저작자를 표시하여야 합니다.



비영리. 귀하는 이 저작물을 영리 목적으로 이용할 수 없습니다.



변경금지. 귀하는 이 저작물을 개작, 변형 또는 가공할 수 없습니다.

- 귀하는, 이 저작물의 재이용이나 배포의 경우, 이 저작물에 적용된 이용허락조건을 명확하게 나타내어야 합니다.
- 저작권자로부터 별도의 허가를 받으면 이러한 조건들은 적용되지 않습니다.

저작권법에 따른 이용자의 권리와 책임은 위의 내용에 의하여 영향을 받지 않습니다.

이것은 [이용허락규약\(Legal Code\)](#)을 이해하기 쉽게 요약한 것입니다.

[Disclaimer](#)



Thesis for the Master of Science

*3D Pose estimation and Evaluation with New  
Calibration Method Based on Lighthouse  
Technology*

*Dongyeon Kim*

Graduate School of Hanyang University

*February 2019*

Thesis for Master of Science

*3D Pose estimation and Evaluation with New Calibration Method  
Based on Lighthouse Technology*

Thesis Supervisor: Prof. Sungon Lee

A Thesis submitted to the graduate school of  
Hanyang University in partial fulfillment of the requirements  
for the degree of *Master of Science*

*Dongyeon Kim*

February 2019

Department of Electrical and Electronic Engineering  
Graduate School of Hanyang University

This thesis, written by Dongyeon Kim,  
has been approved as a thesis for the *Master of Science*.

February 2019



Committee Chairman: Byung-Ju Yi (Signature)

Committee member: Youngjin Choi (Signature)

Committee member: Sungon Lee (Signature)

Graduate School of Hanyang University

# CONTENTS

|   |           |
|---|-----------|
| <b>Abstract</b>                                       | <b>vi</b> |
| <b>1 Introduction</b>                                 | <b>1</b>  |
| <b>2 Architecture</b>                                 | <b>5</b>  |
| 2.1 Architecture . . . . .                            | 6         |
| 2.1.1 Base station Architecture . . . . .             | 6         |
| 2.1.2 Marker Architecture . . . . .                   | 8         |
| <b>3 Methods</b>                                      | <b>11</b> |
| 3.1 Process of the positioning system . . . . .       | 14        |
| 3.1.1 Specific logic . . . . .                        | 15        |
| 3.2 Proposed method . . . . .                         | 19        |
| 3.2.1 Location Determination Problem . . . . .        | 19        |
| 3.2.2 Closed-form solution of absolute pose . . . . . | 23        |
| <b>4 Experiment result</b>                            | <b>29</b> |
| 4.1 Experiment 1 . . . . .                            | 31        |
| 4.2 Experiment 2 . . . . .                            | 40        |
| 4.3 Experiment 3 . . . . .                            | 48        |

|                             |           |
|-----------------------------|-----------|
| <b>5 CONCLUDING REMARKS</b> | <b>52</b> |
| <b>Bibliography</b>         | <b>54</b> |



## **LIST OF FIGURES**

|      |  |    |
|------|--|----|
| 2.1  | System architecture overview . . . . .   | 6  |
| 2.2  | Inside structure of base station . . . . .   | 7  |
| 2.3  | The base stations synchronized flash . . . . .   | 7  |
| 2.4  | The base stations vertical and horizontal laser sweeps . . . . .   | 8  |
| 2.5  | Base station sweep . . . . .   | 8  |
| 3.1  | 7x9 chessboard [1] . . . . .   | 12 |
| 3.2  | Process of proposed method which uses linear stage with two axis and only one sensor. . . . .                                  | 13 |
| 3.3  | Incident planes and lines . . . . .  | 15 |
| 3.4  | General transform of a vector . . . . .  | 16 |
| 3.5  | Transformations of the coordinates . . . . .   | 17 |
| 3.6  | (a) Two vectors are shown in each lighthouse coordinates and (b) Convert lighthouse coordinates to world coordinates . . . . . | 17 |
| 3.7  | The closet points between two lines . . . . .  | 18 |
| 3.8  | Location determination of the points with respect to the lighthouse coordinates  | 20 |
| 3.9  | Proposed method (Move linear stage) . . . . .  | 21 |
| 3.10 | Look at the three points from two different coordinate systems . . . . .   | 24 |
| 3.11 | Example of two different coordinate systems . . . . .  | 25 |

---

|   |    |
|---|----|
| 3.12 Proposed method (make a coordinates) . . . . .   | 28 |
| 4.1 (a) is combined two stage and (b) is system of the experiments . . . . .  | 30 |
| 4.2 Define parameters $\theta_1$ and $\theta_2$ . . . . .   | 32 |
| 4.3 Example of calibration precision . . . . .  | 32 |
| 4.4 Average pose accuracy according to the errors . . . . .   | 34 |
| 4.5 Pose accuracy according to the errors(Specific) . . . . .   | 35 |
| 4.6 Pose accuracy given error 0mm . . . . .   | 36 |
| 4.7 Pose accuracy given error 1mm . . . . .   | 37 |
| 4.8 Pose accuracy given error 3mm . . . . .   | 38 |
| 4.9 Pose accuracy given error 5mm . . . . .   | 39 |
| 4.10 Detecting range of base station and difference between center direction and<br>others( $\theta_1 > \theta_2$ ) . . . . . | 40 |
| 4.11 Sample figure in case1 and case2 . . . . .   | 41 |
| 4.12 Base stations look at the marker . . . . .   | 41 |
| 4.13 Various environment set of case 1 . . . . .  | 43 |
| 4.14 Various environment set of case 2 . . . . .  | 44 |
| 4.15 Various environment set of case 3 . . . . .  | 45 |
| 4.16 Various environment set of case 4 . . . . .  | 46 |
| 4.17 Average pose accuracy above four data . . . . .  | 47 |
| 4.18 System in experiment3 . . . . .  | 48 |
| 4.19 Position accuracy with NDI system . . . . .  | 50 |
| 4.20 Orientation accuracy with NDI system . . . . .   | 51 |

## **LIST OF TABLES**

|     |  |    |
|-----|--|----|
| 2.1 | Sample pulses notation received by a photo sensor module on the marker . . . . . | 8  |
| 4.1 | Setup experiment1 . . . . .  | 33 |
| 4.2 | Experiment 1 result . . . . .  | 33 |
| 4.3 | Setup experiment 2 . . . . .   | 40 |
| 4.4 | Experiment2 result . . . . .   | 42 |
| 4.5 | Setup experiment3 . . . . .  | 48 |
| 4.6 | Experiment3 result . . . . .   | 49 |

# ABSTRACT

## **3D Pose estimation and Evaluation with New Calibration Method Based on Lighthouse Technology**

Dongyeon Kim,  
Dept. of Electrical and  
Electronic Engineering,  
The Graduate School  
Hanyang University

In 2015, Vive is virtual reality system developed by HTC and Valve Corporation. This is a type of an indoor positioning system (IPS) and it based on an infrared laser. To estimate a pose (position and orientation) of an object, an equipment called "lighthouse" or "base station" is used. Presently this IPS attracts much attention as it has low cost compared with other commercial systems as well as high precision and low latency.

Geometry feature points of an object (rigid body) need at least three when measuring the pose of the object with single camera. From that points, the pose with respect to the camera coordinates is able to be estimated by the method of Pnp(Perspective n-points). With two lighthouses, the method of triangulation can be used for estimating the pose like stereo vision of camera system. In order to use the method of triangulation, the relationships of position and rotation between two lighthouses must be known. These relationships are called calibration. A geometric information which is distances among the feature points is used for calibration. If the information contains an error, not just it causes an invalid calibration, but it is impossible to find the accurate pose of the object. Calibration in Vive system requires the object with feature points that are sensors which can detect an infrared ray emitted by lighthouses and exact geometric information among the sensors. These sensors are attached

to the object which is manufactured in person for calibration and pose estimation, such the object is called marker. However, a limitation of this calibration is difficult to measure the exact geometric information due to the error in marker manufacturing, or sensors that attached to the marker.

In this thesis, a new calibration method to obtain accurate geometric information among the sensors has been proposed. The accuracy of the pose estimation according to the information error was verified through experiments. In addition, the pose accuracy of the marker by applying the proposed method is checked and compared it with the commercial system. When the geometrical error of  $5\text{ mm}$  occurs in the calibration, the position is about 6 times and the orientation is about 3 times less accurate than when there is no error. The commercial system estimates the pose of the object very accurately, sometimes errors occurs as it can be sensitive to natural light. Besides the detected area is limited to about  $3\text{ m}^3$ . On the other hand, the lighthouse system is less accurate than the commercial system in terms of the accuracy of the optical axis, but there is no error due to natural light. Also, the detected area is about  $10\text{ m}^3$ . Moreover, it has price competitiveness because of 100 times cheaper than commercial system. In summary, the Vive system can be applied to inexpensive and highly accurate IPS in pose estimation applications where the position and orientation error are allowed more than  $1.5\text{ mm}$  and  $0.3^\circ$ .

## Chapter

# 1

## INTRODUCTION

An indoor positioning system (IPS) is a system to locate objects inside an indoor or a building using lights, radio waves, magnetic fields, acoustic signals, or other sensory information collected by devices [2]. A Vive which is kinds of IPS is virtual reality (VR) system developed by HTC and Valve Corporation in 2015 [3, 4]. The VR system consists of two main parts. The first part of system is a head-mounted display (HMD) which attached lots of photo sensors and inertial measurement unit (IMU). Another part of system is a base station("lighthouse") which emits two patterns of infrared ray. The HMD detects infrared ray pulses emitted by base stations to determine its pose in a space with respect to world coordinates. The main of a tracking system is to detect pose of an object which have the six degrees of freedom (DoF). The most fundamental and important things of the tracking system are accurate and stable positioning. The merit of laser-based positioning system has a precise and reliable tracking with low cost and low latency. Moreover, a range of the tracking is wide about  $20m^2$  and low price below 1 thousand US dollars. On the other hand, the vision based optical tracking system developed by NDI [5] also can have precise and stable tracking but a range of the tracking has limited and a high price above 20 thousand

US dollars.

Although history of the positioning system with Vive is not as long as with a camera, its study and application are active. Cuervo[6] compared various VR devices contained Vive from the point of view of normal users, not the researchers. The result of a quantitative test for accuracy and precision of pose tracking as well as system latency showed in Vive system [7]. Maciejewski et al.[8] attached the markers of Vive and Optitrack that is multi-camera motion capturing system to a same object, and measured the pose error and pose jitter in a setup range. Quiñones et al.[9] developed their own tracking device that is more small, light and cheap than commercial tracker. Moreover, accuracy comparison between commercial controller and developed device confirm an accuracy performance.

Pose estimation is referred to as the perspective n-points problem (PnP) have been long studied and most of its methods is to estimate the pose of the calibrated camera from 3D world coordinate points to 2D image points correspondences [10]. In case of more than 6 control points, the PnP problem can be solved by the direct linear transformation (DLT) [11] and has a unique linear solution, otherwise it has multiple solutions. When the number of equations more than the variables, the solution of PnP has to solve nonlinear problem. The solutions of nonlinear problems widely divided closed-form solution [12, 13] and iterative optimization solutions [14]. P3P problems [15, 16] and P4P problems [17, 18, 19] have been studied and their solutions can approach various method. Pose estimation algorithm is suggested in case of solving the occlusion problem and the precision of the pose estimation with multiple base station are adjusted [20]. Similar to the Vive system, the both of base station and tracked object is implemented and remained a future work as improvement of the managing the sources of jitter and noise problems whose comes from the unbalance rotors of the base station and vibration mechanical components [21] .

What needs to be done before the pose estimation is a calibration. The calibration in Vive system is to obtain the position and orientation of base stations coordinates with respect to world coordinates. However, most of the previous study used the calibration data given by commercial software, or the explanation of calibration is weak.

This thesis will deal with a new method of calibration to estimate pose in Vive system. Additionally, the result of precision of pose estimation with this method will show by the experiments.

## **Thesis Preview**

Chapter 2 introduces architectures of a base station and own marker. The base station emits two main rays. One is synchronized flash which comes from infrared light matrix, it indicates the start of the system and distinguishes ID between two base stations. Other is horizontal and vertical scanning volumes. It sweeps space and indicates the location of sensors when sensors were contacted by scanning volume. Own marker consists a micro-controller(MCU) and sensor modules. MCU has 48MHz clocks and converting the time to angles of sensors. Sensor modules convert infrared light into digital signal output. In chapter 3, the procedure of pose estimation in Vive system is explained and a new method of calibration has been proposed. Calibration is necessary to estimate the accurate pose of the two coordinate systems. However, it is difficult to measure the exact distance among the location of the all sensors attached to the designed marker due to manufacturing faults in marker and attached sensors. The proposed method used only linear stage and an one sensor. Although the developed method is spending more time as compared to the existing methods, it is robust to manufacturing errors. Chapter 4 shows three parts of the experiment results. First, the evaluations of accuracy of the position and orientation will be examined

with respect to the precision of calibration. Second, the accuracy of pose estimation with proposed the method of calibration in various environmental setup conditions is evaluated. Last, the accuracy of pose estimation in Vive system is evaluated with NDI system that has high accuracy within a range where two systems overlap. With the quantitative comparison between Vive and NDI system, the advantage and disadvantage of the Vive system is explained. Finally, conclusion remarks about this thesis are presented in chapter 5.



# Chapter 2

## ARCHITECTURE

The architecture of the positioning system consists of two components: a base station("Lighthouse") and a tracked object("Marker"). The lighthouse contains three main parts. One is a synchronized flash blinker and others are two rotors. The flash blinker is IR matrix which emits IR pulse in the opposite direction of the optical axis from the lighthouse reference coordinates. Each rotors have high precision rotation speed and make horizontal and vertical scanning volumes through the laser sweeps. The marker consists of a Teensy 3.2, which uses an ARM processor running at 48 MHz and a sensor module(TS3633-CM1) which convert infrared light into digital signal output.

As shown in Figure (2.1), The sensor module will pick up the each signals which are sync flash and horizontal and vertical sweep laser from the two base stations. The teensy calculate signals to time data and use it to distinguish the base stations ID and to determine azimuth and elevation angles of sensor modules with respect to the inverse optical axis of the base stations. After additional operation, the teensy transmits sensors position data to a host PC, which is responsible for calculating the 3D position and orientation of the marker by using a pose estimation algorithm.

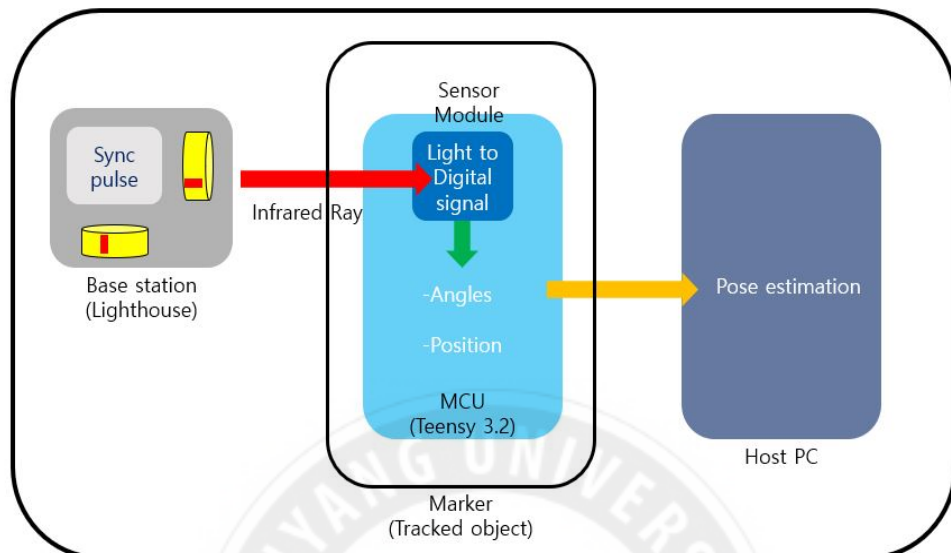


Figure 2.1: System architecture overview

## 2.1 Architecture

### 2.1.1 Base station Architecture

As shown in Figure (2.2), the base station consists of two parts. The first part is sync flash blinker attached IR array which spread infrared ray volume in the direction that the base station looks at. The second part is rotors which make each vertical and horizontal plane in the scan volume with constant rotation speed (120Hz). Rotor1 which makes vertical laser plane rotates around the y-axis, right to left, and Rotor2 makes horizontal laser plane rotates around the x-axis goes bottom to top.

The synchronized flash shows in figure (2.3). what the infrared LED array is emitted means the beginning of a period when the rotor position is at  $0^\circ$  and denoted by  $B_1$  and  $B_2$ . The vertical and horizontal laser sweep can be shown in figure (2.4). The vertical laser

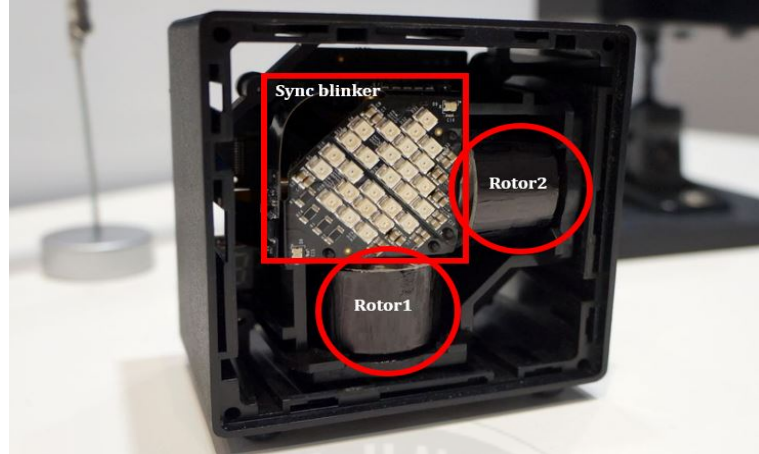


Figure 2.2: Inside structure of base station [22]. The sync blink array which makes sync flash draw in red. The rotors which make each vertical and horizontal plans are circled in red

sweep decides y plane of the detected marker relative to the lighthouse inverse optical axis and denoted by  $R_1$ . The horizontal laser sweep decides x plane of the detected marker with respect to same axis above and denoted by  $R_2$ . Both rotor  $R_1$  and  $R_2$  are rotated the same RPM(60Hz) and their relative phase is at  $180^\circ$ .  $B_1$  and  $B_2$  have different duration of the pulse which can be distinguished base stations.

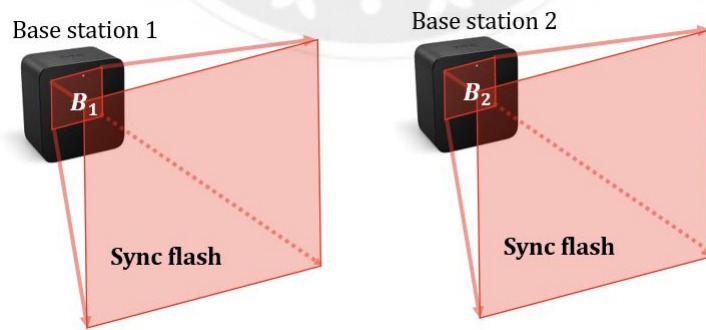


Figure 2.3: The base stations synchronized flash

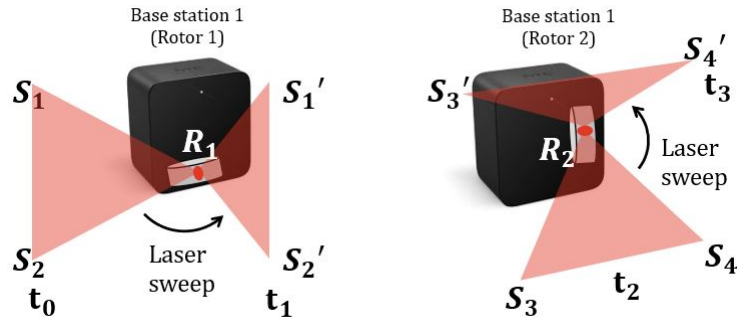


Figure 2.4: The base stations vertical and horizontal laser sweeps

### 2.1.2 Marker Architecture

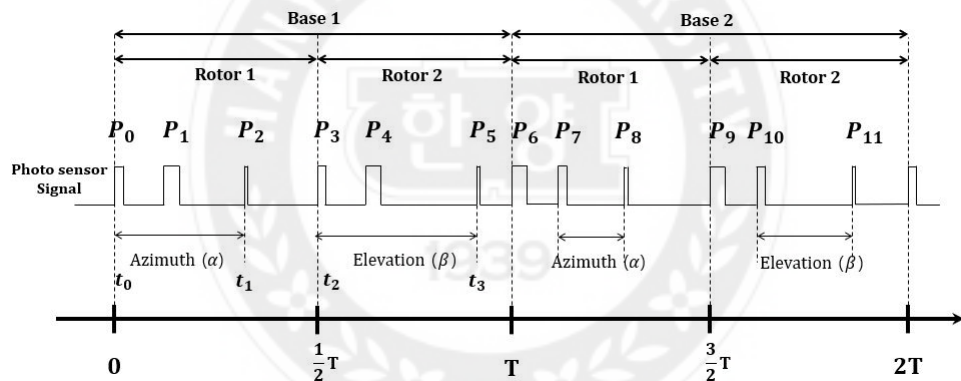


Figure 2.5: Sample pulses notation received by a photo sensor module on the marker

|             | Rotors       | Synchronized pulse      | vertical sweep pulse | horizontal sweep pulse |
|-------------|--------------|-------------------------|----------------------|------------------------|
| Lighthouse1 | $R_1, R_2$   | $P_0, P_3, P_6, P_9$    | $P_2$                | $P_5$                  |
| Lighthouse2 | $R'_1, R'_2$ | $P_1, P_4, P_7, P_{10}$ | $P_8$                | $P_{11}$               |

Table 2.1: Sample pulses notation received by a photo sensor module on the marker

- The rotors of the base station 1 are denoted by  $R_1$  and  $R_2$
- The rotors of the base station 2 are denoted by  $R'_1$  and  $R'_2$

- The sync pulse from the base station 1 are denoted by  $P_0, P_3, P_6$ , and  $P_9$ .
- The sync pulse from the base station 2 are denoted by  $P_1, P_4, P_7$ , and  $P_{10}$ .
- The vertical and horizontal sweep pulses from the base station 1 are each  $P_2$  and  $P_5$
- The vertical and horizontal sweep pulses from the base station 2 are each  $P_8$  and  $P_{11}$
- Period ( $T$ ) is  $16.666[ms]$  and all system update rate is  $30Hz$  ( $2T * 30Hz \approx 1[sec]$ )

The example signal sequence is shown in figure (2.5) and explain the notation in table (2.1).The difference pulses duration as  $P_0$  and  $P_1$  or  $P_6$  and  $P_5$  can distinguish the base station ID in the sync pulses. And the difference pulse duration like  $P_0$  and  $P_3$  indicates whether following signal will be vertical sweep or horizontal sweep.

The pulses  $P_0$  and  $P_1$  emitted by  $B_1$  and  $B_2$  when the vertical laser plane of the base station 1 is at  $0^\circ$  and these pulses are simultaneously received by all sensor modules. The pulse  $P_2$  is received when the vertical laser scan line from  $\overline{S_1S_2}$  at  $t_0$  to  $\overline{S'_1S'_2}$  at  $t_1$ . Same as, The pulses  $P_3$  and  $P_4$  emitted by  $B_1$  and  $B_2$  when the horizontal plane is at  $0^\circ$  for the horizontal laser line of each base station rotors  $R_2$  and  $R'_2$ . Also, The pulse  $P_5$  is received when the horizontal laser scan line from  $\overline{S_3S_4}$  at  $t_2$  and  $\overline{S'_3S'_4}$  at  $t_3$ .

All sweep lasers except sync blink from the base station 2 turns off during the laser sweep by base station 1 rotor( $R_1$  and  $R_2$ ). That is why relative phase of the two base stations is at  $180^\circ$ .

The relative time between the rising edge of pulse  $P_0$  and  $P_2$  at  $t_0$  and  $t_1$  gives an information when the vertical laser sweep hit the sensors. Also the time difference between the rising edge of pulse  $P_3$  and  $P_5$  at  $t_3$  and  $t_2$  gives the information when the horizontal laser sweep hit the sensors.

The relative time difference express clock ticks. As the teensy is microcontroller runs at 48 MHz, the number of measured clock ticks to time as  $\Delta t = \frac{\text{clock ticks}}{48,000,000}$ . And it takes 8.333ms to laser sweep from 0° to 180°. Therefore, We can convert the difference time between sync pulse and sweep pulse into vertical and horizontal angles with respect to inverse optical axis of base station as follow:

$$\begin{aligned}\theta_v &= \pi \left( \frac{\Delta t - \tau}{T/2} \right) \\ \theta_h &= \pi \left( \frac{\Delta t - \tau}{T/2} \right)\end{aligned}\tag{2.1}$$

where  $\theta_v$  and  $\theta_h$  are vertical and horizontal angles relative to base station optical axis,  $\tau (= 4000)$  is center time and  $T (= 16.333\text{ms})$  is period.

In the same process above, we can get the angles of vertical and horizontal about base station 2.

# Chapter 3

## METHODS

In this chapter, the method of a pose estimation and proposed method will be mentioned.

The pose estimation is that to estimate pose of object with respect to reference or world coordinates in the camera system. Typical methods of pose estimation are perspective n-points and triangulation. Moreover, the step that must be taken before using this method is a calibration. The result of the calibration is to obtain the intrinsic and extrinsic parameters [23].

Intrinsic parameters consist of focal length, principle points, skew factor, distortion and so on to find the quantities internal to the camera that affect the imaging process. What we are interested in is extrinsic parameters which present not only the location of the camera in the 3D space but also absolute pose in case of multiple camera, stereo camera.

Almost camera calibration is based on a camera pinhole model theory [24] and use a tool like chessboard in figure (3.1). The merit of this tool has regular with high precision length and location of each corner points is constant. As the number of corner points(input value) increases, the result of calibration becomes more accurate. This calibration method can cause the high precision of pose estimation.

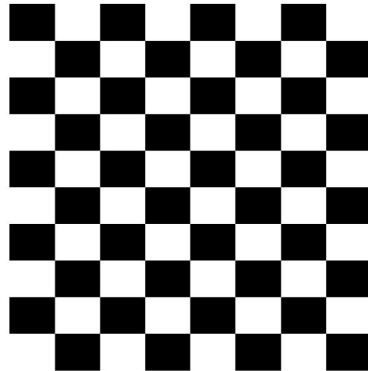


Figure 3.1: 7x9 chessboard [1]

Likewise, the calibration to find extrinsic parameters is important component to estimate pose in Vive system. The result of the calibration is the position and orientation of base station with respect to world coordinates.

Calibration process in Vive system, a component is to estimate the relative distances of sensors. However, it is difficult to obtain the relative distances of each sensors on designed marker. Besides manufactured errors also exist. The more accurate the calibration, the more accurate the measurement.

We proposed a new method of calibration in Vive system. Only one sensor and linear stage tool are used. Unless a fixed lighthouse is moved, calibration is only performed once. There are two steps in this process as follow:

1. A sensor attached to linear stage is measured in each lighthouses
2. Record data and Move the stage by the desired direction and displacement
3. Iterative 1-2, three times
4. Calculate pose of marker with respect to world coordinates

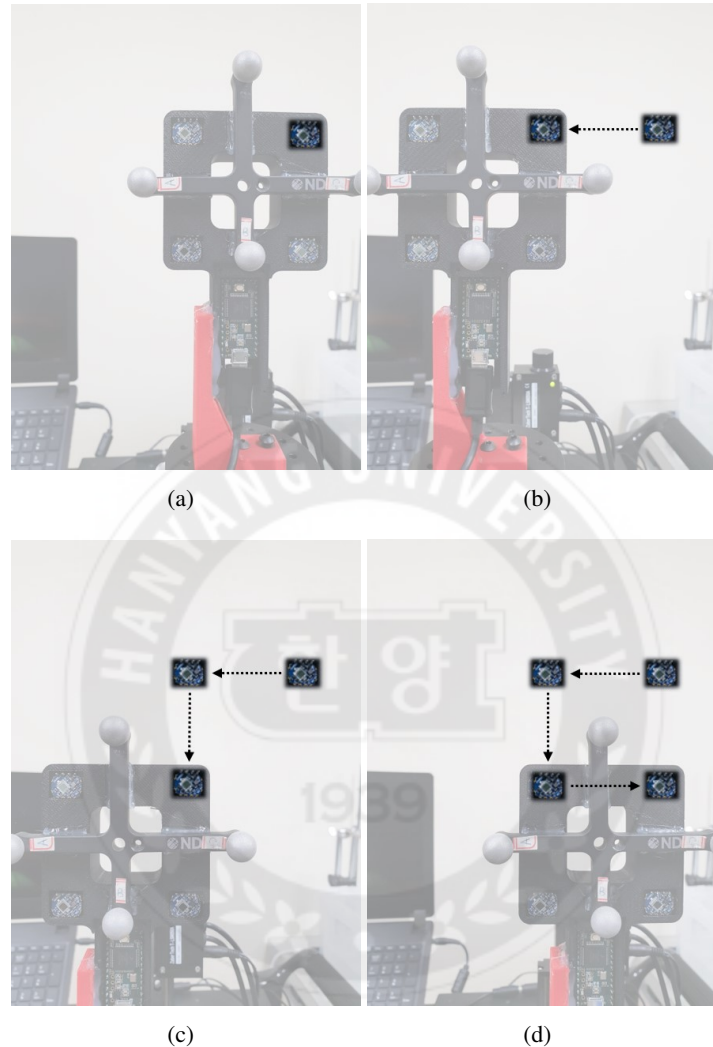


Figure 3.2: Process of proposed method which uses linear stage with two axis and only one sensor.

In this proposed method, move the stage at least two direction to make coordinates. If not, the sensor can not make coordinates. The advantage of this method is to obtain the precision location of moved the sensor. Therefore the precision lengths are known and has

robust in the manufacture errors. It makes a result in correct calibration. However, weakness of this system is it takes a long time and need the linear stage which has high precision.

To implement this method, the location determination problem (LDP) [12] or perspective four points problem [17] and closed-form solution have to be solved. Through this process, the result is that the position and orientation of marker coordinates with respect to world coordinates.

### **3.1 Process of the positioning system**

The positioning of Vive system well explained in [25] and their process is available in Arduino using a program called Teensyduino [26]. Process shows as follow:

1. Each base stations emit three patterns of infrared ray
2. All sensor modules get the different patterns ray and convert its pulses to angles following time
3. Calculate the unit vectors from base stations to sensors
4. Change the base station coordinates of each unit vectors into the world coordinates
5. Obtain the closet points of two lines which come from the converted unit vectors
6. Estimate the position and orientation of marker with four position of sensors with respect to the world coordinates

### 3.1.1 Specific logic

#### Measure the angles

From the equation (2.1), We measured the angles of the sensors.

#### Incident planes and lines

The “incident plane” is the plane defined by the angle between a sensor and a lighthouse (3.3). From the cross product of the normal vectors of two incident planes, a vector(“incident line”) between the marker and the lighthouse is defined [9].

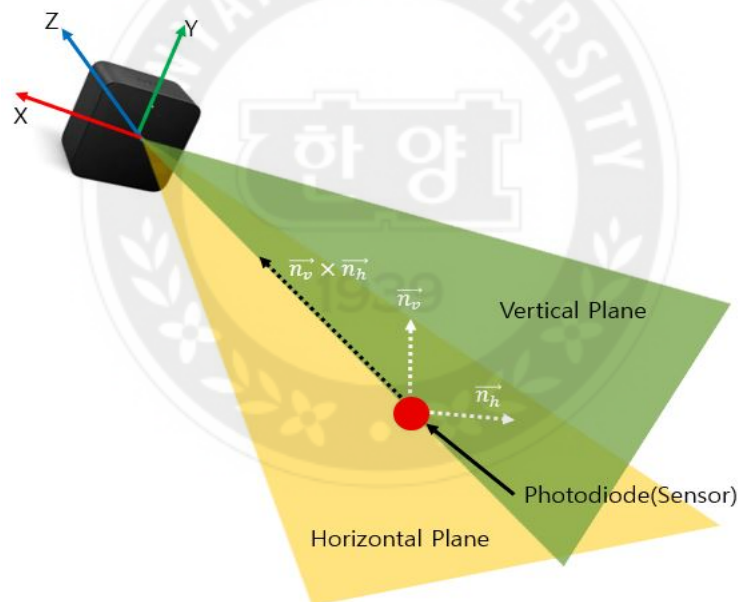


Figure 3.3: Incident planes and lines

### Convert coordinates

The incident lines from the each lighthouses convert into the marker coordinate. To know the absolute pose of each lighthouses, the calibration(3.2) is necessary to convert two lines.

Mapping the description of a vector with respect to frame B, and we would like to know its description with respect to another frame,A in figure(3.4) [27].

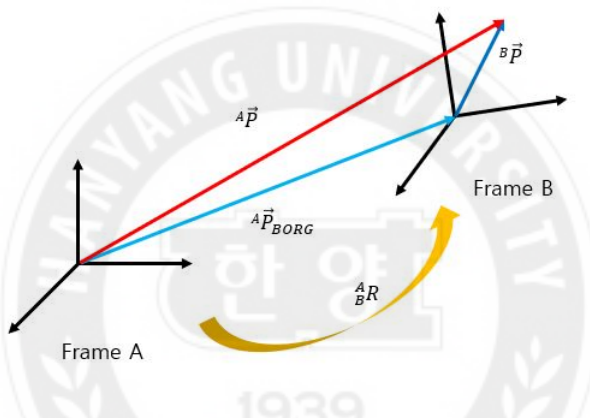


Figure 3.4: General transform of a vector

where  ${}^A_R$  is rotation of B coordinates system with respect to A coordinates system ,  ${}^A P_{BORG}$  is vector of A frame origin to B frame origin ,  ${}^A P$  is vector expressed by A coordinates,  ${}^B P$  is vector expressed by B coordinates. as follow:

$${}^A P = {}^A P_{BORG} + {}^A R {}^B P \quad (3.1)$$

In the result of the calibration, the absolute pose of each lighthouses is obtained in figure (3.5).

The incident vectors are presented in base station coordinates, and changed its coordi-

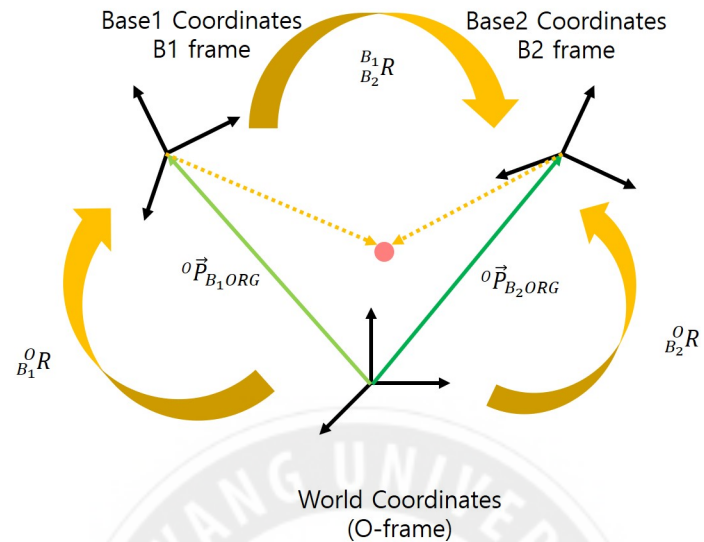


Figure 3.5: Transformations of the coordinates

nates to world coordinates in the figure (3.6).

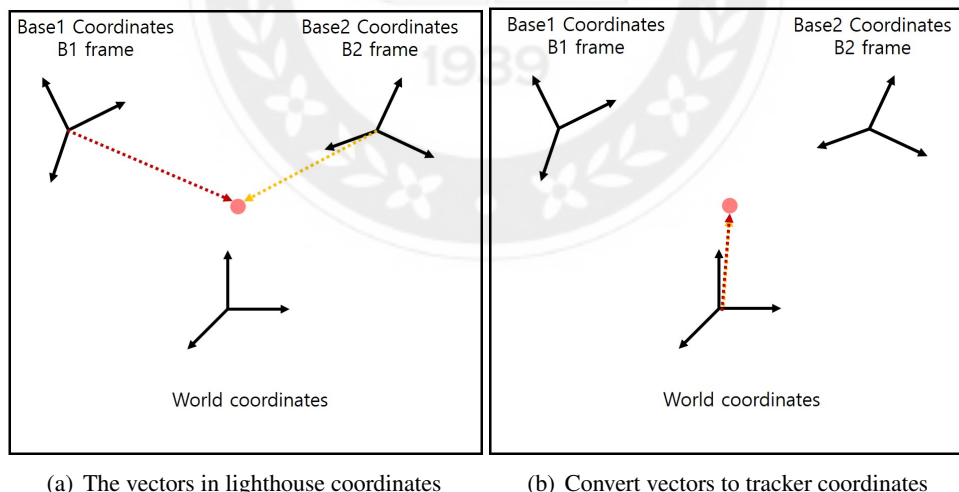


Figure 3.6: (a) Two vectors are shown in each lighthouse coordinates and (b) Convert lighthouse coordinates to world coordinates

### The closet point of two lines

Find the closet points of two lines that convert each vectors from base station to the same coordinates. It can be easily solved when two lines that convert vectors from lighthouse to the same coordinates are intersected. If not, two lines are parallel, the closet point of two lines have to be solved [28].

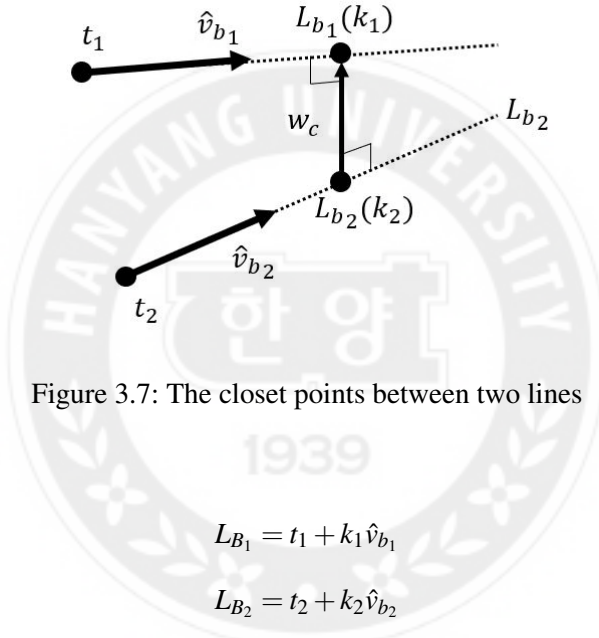


Figure 3.7: The closet points between two lines

$$\begin{aligned} L_{B_1} &= t_1 + k_1 \hat{v}_{b_1} \\ L_{B_2} &= t_2 + k_2 \hat{v}_{b_2} \end{aligned} \quad (3.2)$$

where the unit vectors are  $\hat{v}_{b_1}, \hat{v}_{b_2}$ , the origins of two coordinates  $t_1, t_2$  and unknown variables are  $k_1, k_2$ .

To solve the closet point of two lines, the length of vector  $\vec{\omega}_c$  is minimized.

$$\vec{\omega}_c = L_{B_1} - L_{B_2} \quad (3.3)$$

Also, the vector of  $\vec{\omega}_c$  is uniquely perpendicular to two unit vectors  $\hat{v}_{b_1}$  and  $\hat{v}_{b_2}$ , and two equations are satisfied according to the perpendicular characteristic.

$$\begin{aligned}\hat{v}_{b_1} \cdot \vec{\omega}_c &= 0 \\ \hat{v}_{b_2} \cdot \vec{\omega}_c &= 0\end{aligned}\tag{3.4}$$

### Pose estimation

Positions of the four sensors, the result of the previous steps, consist of the marker coordinates. Specific logic will show in section (3.2.2).

## 3.2 Proposed method

What we proposed method is that calibration method to find absolute pose of light-houses, it needs in the process section (3.1-4) when converting coordinates. In previous studies for the Vive system, almost used the calibration data given by commercial software using HMD. Otherwise, calibration was performed using a marker set in person. The calibration process need the distance among the sensors. Error occurs when manufacturing marker or attaching sensors to designed marker.

### 3.2.1 Location Determination Problem

After processing in figure 3.2, a stage used to move one sensor and made a shape like four sensors attached to a designed marker.

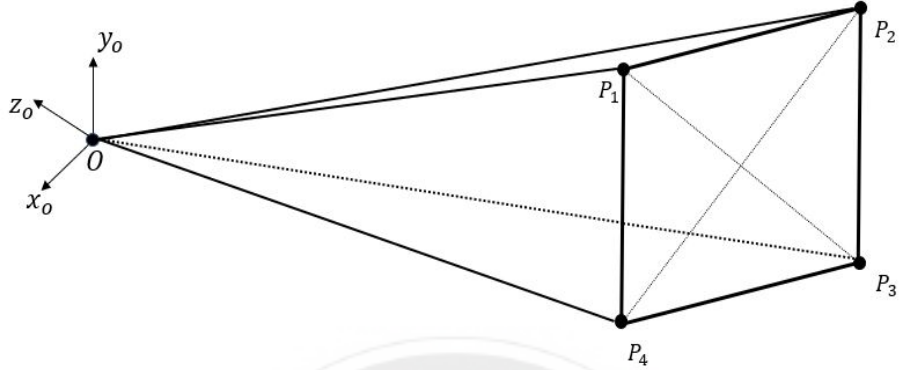


Figure 3.8: Location determination of the points with respect to the lighthouse coordinates

Let  $L_1 = \overline{OP_1}$ ,  $L_2 = \overline{OP_2}$ ,  $L_3 = \overline{OP_3}$ ,  $L_4 = \overline{OP_4}$ ,  $\angle(P_1OP_2) = \theta_{12}$ ,  $\angle(P_1OP_3) = \theta_{13}$ ,  $\angle(P_1OP_4) = \theta_{14}$ ,  $\angle(P_2OP_3) = \theta_{23}$ ,  $\angle(P_3OP_4) = \theta_{34}$

From triangles  $CP_1P_2$ ,  $CP_1P_3$ ,  $CP_1P_4$ ,  $CP_2P_3$ ,  $CP_2P_4$  and  $CP_3P_4$ , we can obtain equations by the law of cosin as follow:

$$\begin{cases} L_1^2 + L_2^2 - 2L_1L_2\cos\theta_{12} - |P_1P_2|^2 = 0 \\ L_1^2 + L_3^2 - 2L_1L_3\cos\theta_{13} - |P_1P_3|^2 = 0 \\ L_1^2 + L_4^2 - 2L_1L_4\cos\theta_{14} - |P_1P_4|^2 = 0 \\ L_2^2 + L_3^2 - 2L_2L_3\cos\theta_{23} - |P_2P_3|^2 = 0 \\ L_2^2 + L_4^2 - 2L_2L_4\cos\theta_{24} - |P_2P_4|^2 = 0 \\ L_3^2 + L_4^2 - 2L_3L_4\cos\theta_{34} - |P_3P_4|^2 = 0 \end{cases} \quad (3.5)$$

where each distances between two points such as  $|P_1P_2|$ ,  $|P_1P_3|$ ,  $|P_1P_4|$ ,  $|P_2P_3|$ ,  $|P_2P_4|$  and  $|P_3P_4|$  are known as measurement. And  $\cos\theta$  values are computed by the dot product of

each unit vectors. The number of variables is four( $L_1, L_2, L_3$  and  $L_4$ ), while the number of the equations is six. This is overdetermined system. Therefore, nonlinear equation system need to be solved numerically. We used the method of 'Levenberg-Marquardt-Fletcher(LMF) algorithm' [29] to solve nonlinear equation.

### Example

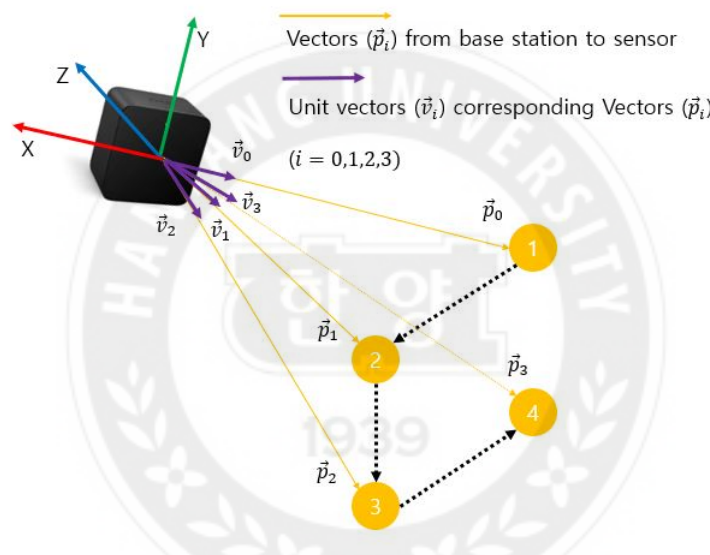


Figure 3.9: Proposed method (Move linear stage)

The proposed method shows in figure (3.9), A number in yellow circle which is a sensor indicate the process order. When number 1, estimate the unit vector via angles in section (3.1.1). Record the unit vector data and move the linear stage to number 2. The moving direction and distance are known and estimate same as above process.

The recorded unit vectors from lighthouse origin to the sensors are estimated from the

equation:

$$\hat{v} = \frac{\vec{v}}{|v|} \quad (3.6)$$

The four position vectors in the lighthouse frame denoted by:

$$\vec{p}_0 = k_0 \hat{v}_0 \quad \vec{p}_1 = k_1 \hat{v}_1 \quad \vec{p}_2 = k_2 \hat{v}_2 \quad \vec{p}_3 = k_3 \hat{v}_3 \quad (3.7)$$

The relative distance and direction are known variables.

$$\begin{aligned} r_{01} &= |\vec{p}_0 - \vec{p}_1| & r_{02} &= |\vec{p}_0 - \vec{p}_2| \\ r_{03} &= |\vec{p}_0 - \vec{p}_3| & r_{12} &= |\vec{p}_1 - \vec{p}_2| \\ r_{13} &= |\vec{p}_1 - \vec{p}_3| & r_{23} &= |\vec{p}_2 - \vec{p}_3| \end{aligned} \quad (3.8)$$

Above them, one equation is solved.

$$\begin{aligned} r_{01}^2 &= |\vec{p}_0 - \vec{p}_1|^2 \\ &= |k_0 \hat{v}_0 - k_1 \hat{v}_1|^2 \\ &= (k_0 v_{0x} - k_1 v_{1x})^2 + (k_0 v_{0y} - k_1 v_{1y})^2 + (k_0 v_{0z} - k_1 v_{1z})^2 \\ &= k_0^2 v_{0x}^2 + k_1^2 v_{1x}^2 - 2k_0 k_1 v_{0x} v_{1x} \\ &\quad + k_0^2 v_{0y}^2 + k_1^2 v_{1y}^2 - 2k_0 k_1 v_{0y} v_{1y} \\ &\quad + k_0^2 v_{0z}^2 + k_1^2 v_{1z}^2 - 2k_0 k_1 v_{0z} v_{1z} \\ &= k_0^2 (v_{0x}^2 + v_{0y}^2 + v_{0z}^2) + k_1^2 (v_{1x}^2 + v_{1y}^2 + v_{1z}^2) \\ &\quad - 2k_0 k_1 (v_{0x} v_{1x} + v_{0y} v_{1y} + v_{0z} v_{1z}) \\ &= k_0^2 |\hat{v}_0|^2 + k_1^2 |\hat{v}_1|^2 - 2k_0 k_1 (\hat{v}_0 \cdot \hat{v}_1) \\ &= k_0^2 + k_1^2 - 2k_0 k_1 (\hat{v}_0 \cdot \hat{v}_1) \end{aligned} \quad (3.9)$$

Same as equation (3.9), equations (3.8) are solved.

$$\begin{cases} k_0^2 + k_1^2 - 2k_0k_1(\hat{v}_0 \cdot \hat{v}_1) - r_{01}^2 = 0 \\ k_0^2 + k_2^2 - 2k_0k_2(\hat{v}_0 \cdot \hat{v}_2) - r_{02}^2 = 0 \\ k_0^2 + k_3^2 - 2k_0k_3(\hat{v}_0 \cdot \hat{v}_3) - r_{03}^2 = 0 \\ k_1^2 + k_2^2 - 2k_1k_2(\hat{v}_1 \cdot \hat{v}_2) - r_{12}^2 = 0 \\ k_1^2 + k_3^2 - 2k_1k_3(\hat{v}_1 \cdot \hat{v}_3) - r_{13}^2 = 0 \\ k_2^2 + k_3^2 - 2k_2k_3(\hat{v}_2 \cdot \hat{v}_3) - r_{23}^2 = 0 \end{cases} \quad (3.10)$$

Get the four unknown variables  $k_0, k_1, k_2, k_3$  using 'LMF algorithm'.

### 3.2.2 Closed-form solution of absolute pose

As shown in Figure (3.10), the coordinates of a number of points at least three as measured between two different coordinates is known, we can find the transformation of two coordinate systems that come from the closed-form solution of absolute orientation expressed by unit quaternions [12].

In case of three points, if the points are in the frmae A, virtual coordinate(A) is made like in figure(3.11).

Let  ${}^B_1 P$  is  $P_1$  vector with respect to frame B and the origin of the frame A. Set the new  $x$  axis from the origin to  ${}^B_2 P$ .

$${}^A \mathbf{x} = {}^B_2 P - {}^B_1 P \quad , \quad {}^A \hat{\mathbf{x}} = \frac{{}^B \mathbf{x}}{\| {}^B \mathbf{x} \|} \quad (3.11)$$

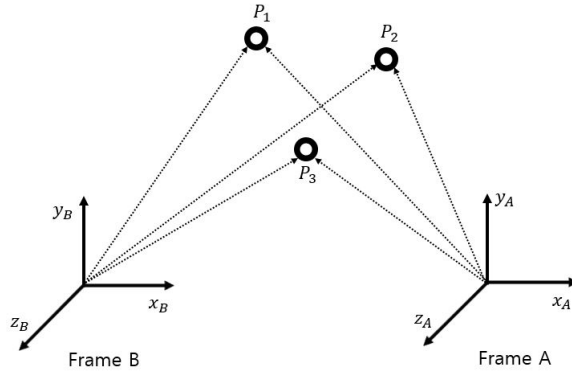


Figure 3.10: Look at the three points from two different coordinate systems

Now let

$${}^B_A\mathbf{y} = ({}^A_3\mathbf{P} - {}^A_1\mathbf{P}) - [({}^A_3\mathbf{P} - {}^A_1\mathbf{P}) \cdot {}^B_A\hat{\mathbf{x}}] {}^B_A\hat{\mathbf{x}}, \quad {}^B_A\hat{\mathbf{y}} = \frac{{}^B_A\mathbf{y}}{\|{}^B_A\mathbf{y}\|} \quad (3.12)$$

From the cross product

$${}^B_A\hat{\mathbf{z}} = {}^B_A\hat{\mathbf{x}} \times {}^B_A\hat{\mathbf{y}} \quad (3.13)$$

The rotation matrix the frame A with respect to the frame B as follow:

$${}^B_A\mathbf{R} = \begin{bmatrix} {}^B_A\hat{\mathbf{x}} & {}^B_A\hat{\mathbf{y}} & {}^B_A\hat{\mathbf{z}} \end{bmatrix} \quad (3.14)$$

### The rotation expressed by unit quaternions

The rotation expressed by unit quaternions can be found when the points are more than three. Set a center of measured points in each coordinates.

$${}^A\bar{\mathbf{P}}_c = \frac{1}{n} \sum_{i=1}^n {}^A_i\mathbf{P}, \quad {}^B\bar{\mathbf{P}}_c = \frac{1}{n} \sum_{i=1}^n {}^B_i\mathbf{P} \quad (3.15)$$

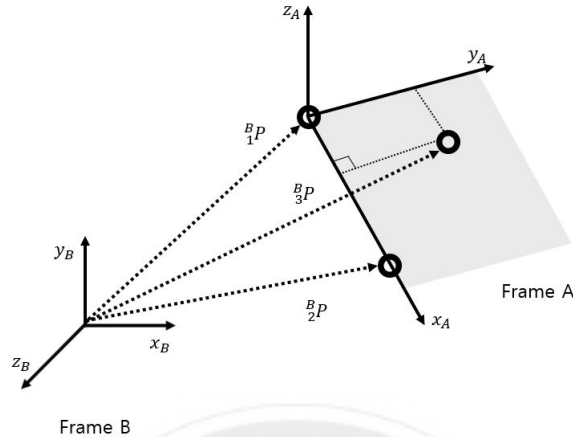


Figure 3.11: Example of two different coordinate systems

Let the new coordinates by

$${}_i^A \mathbf{P}' = {}_i^A \mathbf{P} - {}^A \bar{\mathbf{P}}_c \quad , \quad {}_i^B \mathbf{P}' = {}_i^B \mathbf{P} - {}^B \bar{\mathbf{P}}_c \quad (3.16)$$

Note that

$$\sum_{i=1}^n {}_i^A \mathbf{P}' = 0 \quad , \quad \sum_{i=1}^n {}_i^B \mathbf{P}' = 0 \quad (3.17)$$

The elements of matrix  $M$  are sums of products of coordinates measured in the frame A with coordinates measured in the frame B.

$$M = \sum_{i=1}^n {}_i^A \mathbf{P}' {}_i^B \mathbf{P}'^T \quad (3.18)$$

We write the elements of matrix  $M$

$$M = \begin{bmatrix} S_{xx} & S_{xy} & S_{xz} \\ S_{yx} & S_{yy} & S_{yz} \\ S_{zx} & S_{zy} & S_{zz} \end{bmatrix} \quad (3.19)$$

$$\text{where } S_{xx} = \sum_{i=1}^n {}^A_i \mathbf{x}'^B \mathbf{x}' \quad S_{xy} = \sum_{i=1}^n {}^A_i \mathbf{x}'^B \mathbf{y}' \quad S_{xz} = \sum_{i=1}^n {}^A_i \mathbf{x}'^B \mathbf{z}'$$

Then the 10 independent elements of the real symmetric  $4 \times 4$  matrix  $N$  and differences of the nine elements of the  $3 \times 3$  matrix  $M$ . Note that the trace is zero.

$$N = \begin{bmatrix} N_{11} & N_{12} & N_{13} & N_{14} \\ N_{21} & N_{22} & N_{23} & N_{24} \\ N_{31} & N_{32} & N_{33} & N_{34} \\ N_{41} & N_{42} & N_{43} & N_{44} \end{bmatrix} \quad (3.20)$$

where

$$\begin{aligned} N_{11} &= (S_{xx} + S_{yy} + S_{zz}) & N_{12} &= S_{yz} - S_{zy} & N_{13} &= S_{zx} - S_{xz} & N_{14} &= S_{xy} - S_{yx} \\ N_{21} &= S_{yz} - S_{zy} & N_{22} &= (S_{xx} - S_{yy} - S_{zz}) & N_{23} &= S_{xy} + S_{yx} & N_{24} &= S_{zx} + S_{xz} \\ N_{31} &= S_{zx} - S_{xz} & N_{32} &= S_{xy} + S_{yz} & N_{33} &= (-S_{xx} + S_{yy} - S_{zz}) & N_{34} &= S_{yz} + S_{zy} \\ N_{41} &= S_{xy} - S_{yx} & N_{42} &= S_{zx} + S_{xz} & N_{43} &= S_{yz} + S_{zy} & N_{44} &= (-S_{xx} - S_{yy} + S_{zz}) \end{aligned}$$

The unit quaternion that maximizes

$$\dot{\mathbf{q}}^T N \dot{\mathbf{q}} \quad (3.21)$$

is the eigenvector corresponding to the most positive eigenvalue of the matrix  $N$ .

The eigenvalues are the solutions of fourth order polynomial in  $\lambda$ .

$$\det(N - \lambda I) = 0 \quad (3.22)$$

Among the solutions of  $\lambda$ , we have selected the largest positive eigenvalue( $\lambda_m$ ). Then we find the eigenvector,  $\dot{e}_m$ , corresponding the largest positive eigenvalue by solving the homogeneous equation

$$[N - \lambda_m I] \dot{e}_m = 0 \quad (3.23)$$

The unit quaternion obtained from the eigenvector column( $\dot{e}_m$ ) corresponding  $\lambda_m$ .

$$\dot{e}_m = [q_0 \quad q_x \quad q_y \quad q_z]^T \quad (3.24)$$

If  $q_0$  is negative,

$$\begin{aligned} q_0 &= -\dot{e}_m(1, 1) \\ q_x &= -\dot{e}_m(2, 1) \\ q_y &= -\dot{e}_m(3, 1) \\ q_z &= -\dot{e}_m(4, 1) \end{aligned} \quad (3.25)$$

Convert unit quaternions to rotation matrix as follow:

$$R = \begin{bmatrix} (q_0^2 + q_x^2 + q_y^2 + q_z^2) & 2(q_x q_y - q_0 q_z) & 2(q_x q_z + q_0 q_y) \\ 2(q_x q_y + q_0 q_z) & (q_0^2 - q_x^2 + q_y^2 - q_z^2) & 2(q_y q_z - q_0 q_x) \\ 2(q_x q_z - q_0 q_y) & 2(q_y q_z + q_0 q_x) & (q_0^2 - q_x^2 - q_y^2 + q_z^2) \end{bmatrix} \quad (3.26)$$

Also, Translation can be obtain as follow:

$$\mathbf{T} = \bar{\mathbf{r}}_1 - R(\bar{\mathbf{r}}_2) \quad (3.27)$$

Where  $\bar{\mathbf{r}}_1$  is centroid vector of frame A and  $\bar{\mathbf{r}}_2$  is centroid vector of frame B.

As a result, transformation of the frame A with respect to the frame B is known.

### Example

From the section (3.2.1), the positions with respect to lighthouse can be obtained and also the directions and absolute displacements of sensor are known. Coordinates of sensor is made in figure (3.12).

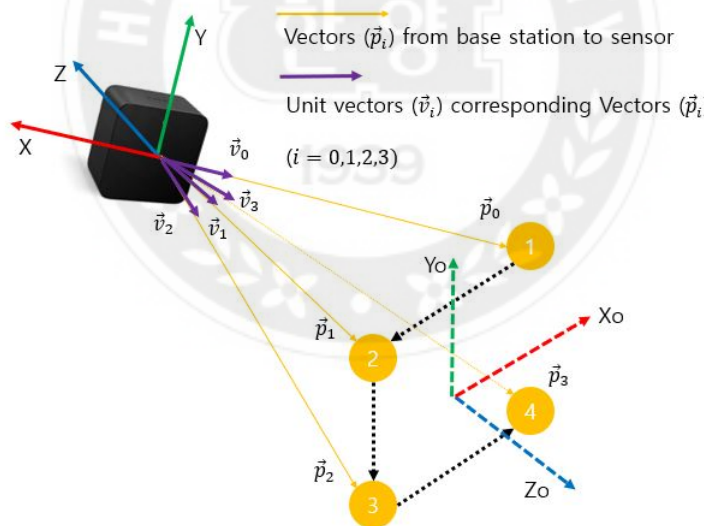


Figure 3.12: Proposed method (make a coordinates)

From the section (3.2.2) with positions, find the absolute pose(calibration) is complete.

# Chapter 4

## EXPERIMENT RESULT

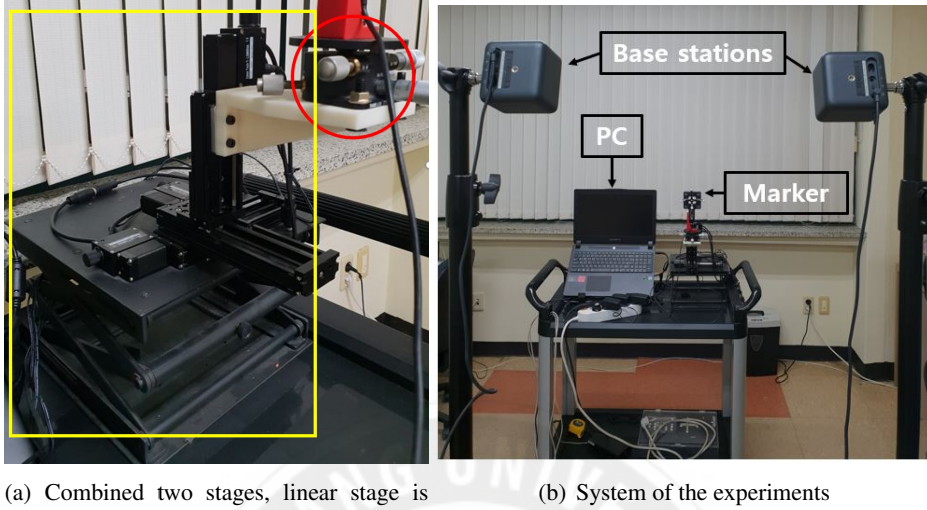
There are three experiment results:

1. Evaluation of pose estimation accuracy according to the geometry information error
2. Evaluation of pose estimation accuracy with proposed method
3. Evaluation of pose estimation accuracy compared with commercial system

Combined an automatic three axis linear stage with a manual rotation stage and system for experiment setup are shown in figure (4.1).

The range of linear stage is x and z direction are 100mm and y direction is 50mm. The range of rotation stage is roll and pitch direction are  $\pm 5^\circ(10^\circ)$  and yaw direction  $\pm 10^\circ(20^\circ)$ .

We conducted an experiment 1 and experiment 2 in space (2m, 2.5m, 3m, 3.5m, 4m, 4.5m from the lighthouses set), then move x, y and z directions and rotate roll, pitch and yaw direction with respect to stage coordinates in each distances. In case of estimating position, linear stage moved 10 steps, one step is 10mm. When estimating rotation, Roll and pitch direction rotate 4 steps (one step is  $1.78^\circ$ ) and yaw direction rotate 13 steps (one step is



(a) Combined two stages, linear stage is drawn in yellow box and rotation stage circled in red

(b) System of the experiments

Figure 4.1: (a) is combined two stage and (b) is system of the experiments

$1.5^\circ$ ). In comparison with NDI system, experiment 3, the pose estimation is process in area where two systems overlap. The amount of movement or rotation same above.

All data get 1000 for each distances and directions and the amount of movement or rotation is used to calculate an error. We defined absolute error of position as follow:

$$E_p = \left| \sqrt{(P_i - P_{i+1})^2} - A \right| \quad (4.1)$$

where  $P_{i+1} = [x_{i+1}, y_{i+1}, z_{i+1}]^T$  is current position,  $P_i = [x_i, y_i, z_i]^T$  is previous position and  $A = 10$  here, and error unit is  $mm$ .

As Rotation express unit quaternions, we can obtain absolute angles between two unit quaternions [12].

$$\theta = \cos^{-1}(2 \langle q_i, q_{i+1} \rangle^2 - 1) \quad (4.2)$$

where  $q_{i+1}$  is current unit quaternion and  $q_i$  is previous unit quaternion, symbol of  $<,>$  is dot product.

We defined absolute error of orientation as follow:

$$E_o = \begin{cases} |\cos^{-1}(2 < q_i, q_{i+1} >^2 - 1) - B|, & \text{if roll and pitch directions} \\ |\cos^{-1}(2 < q_i, q_{i+1} >^2 - 1) - C|, & \text{if yaw direction} \end{cases} \quad (4.3)$$

where  $B = 1.78$  and  $C = 1.5$  here, and error unit is degree( $^\circ$ ).

The experiment parameters defined as follow:

- Height

Base station and marker set height

- Baseline

The distance between two base stations

- $\theta_1$

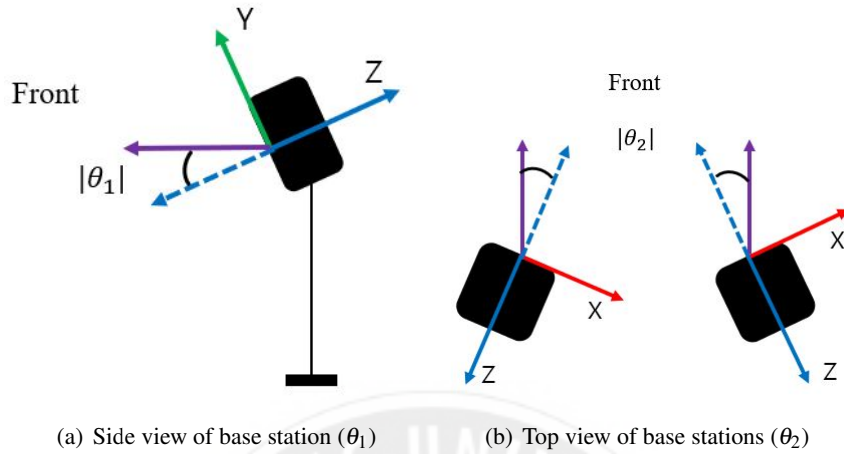
Rotate inverse x-axis about base station coordinates look at downside

- $\theta_2$

Two base stations look at in front of inside direction. Left base station rotate inverse y-axis and Right base station rotate y-axis

## 4.1 Experiment 1

Experiment 1 will show an evaluation of pose estimation accuracy according to the calibration precision. The calibration precision define Converting coordinates is main part of system process to use pose estimation algorithm denoted by section (3.1.1).

Figure 4.2: Define parameters  $\theta_1$  and  $\theta_2$ 

The calibration error defined manufacture marker error, it indicates the error that may occur during the marker manufacturing. That is, the distances and directions between sensors attached to marker is equal to move a sensor attached to linear stage and the calibration error defined its movement move more or less than we set in the figure (4.3).

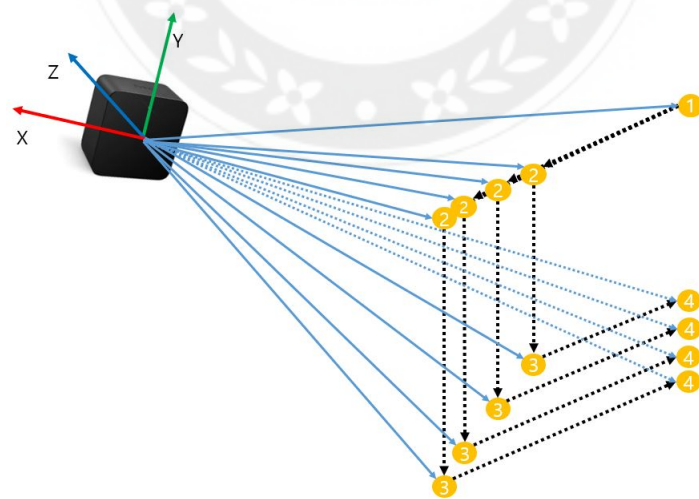


Figure 4.3: Example of calibration precision

| Base station set |          |            |            | Marker |
|------------------|----------|------------|------------|--------|
| Height           | Baseline | $\theta_1$ | $\theta_2$ | Height |
| 1.7m             | 1m       | 10°        | 20°        | 0.95m  |

Table 4.1: Setup experiment1

Given the parameters in table (4.1) and errors are given each 0mm, 1mm, 3mm, 5mm when calibration process. From the results, it allows about 1mm of error. The results of experiment 1 show in table (4.2).

If we are not given the error, average errors of position and orientation are 0.6065mm and 0.2357°. When given error is 1mm, the performance is as good as the error is not given, it allows 1mm of error. While, the error clearly begins to increase when given error is 3mm. In case of the given 5mm error, the position error is 3.5633mm and the orientation error is 0.6981°, it is about six times and three times larger than without error.

The Vive system has a relatively large error with respect to the optical axis,z-axis, compared to the x and y-axis. Therefore, the direction of roll and yaw containing the z-axis component is relatively large in error compared with the pitch direction which contain less z-axis component. As we can see the figure (4.8), Vive system is not always stable.

| Error | Position [mm] |        |        |         | Orientation [°] |        |        |         |
|-------|---------------|--------|--------|---------|-----------------|--------|--------|---------|
|       | x-axis        | y-axis | z-axis | Average | roll            | pitch  | yaw    | Average |
| 0 mm  | 0.3300        | 0.2449 | 1.2446 | 0.6065  | 0.2504          | 0.2290 | 0.2277 | 0.2357  |
| 1 mm  | 0.3371        | 0.3118 | 1.2502 | 0.6330  | 0.2701          | 0.2135 | 0.1333 | 0.2056  |
| 3 mm  | 2.1006        | 2.0914 | 4.8669 | 3.0196  | 0.7084          | 0.1462 | 0.6317 | 0.4954  |
| 5 mm  | 2.1538        | 2.1298 | 6.4064 | 3.5633  | 1.1186          | 0.2217 | 0.7540 | 0.6981  |

Table 4.2: Experiment 1 result

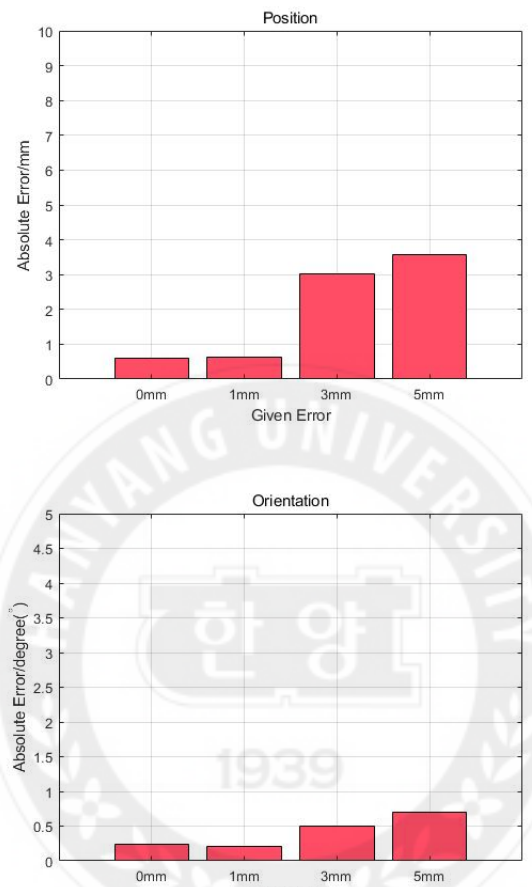


Figure 4.4: Average pose accuracy according to the errors

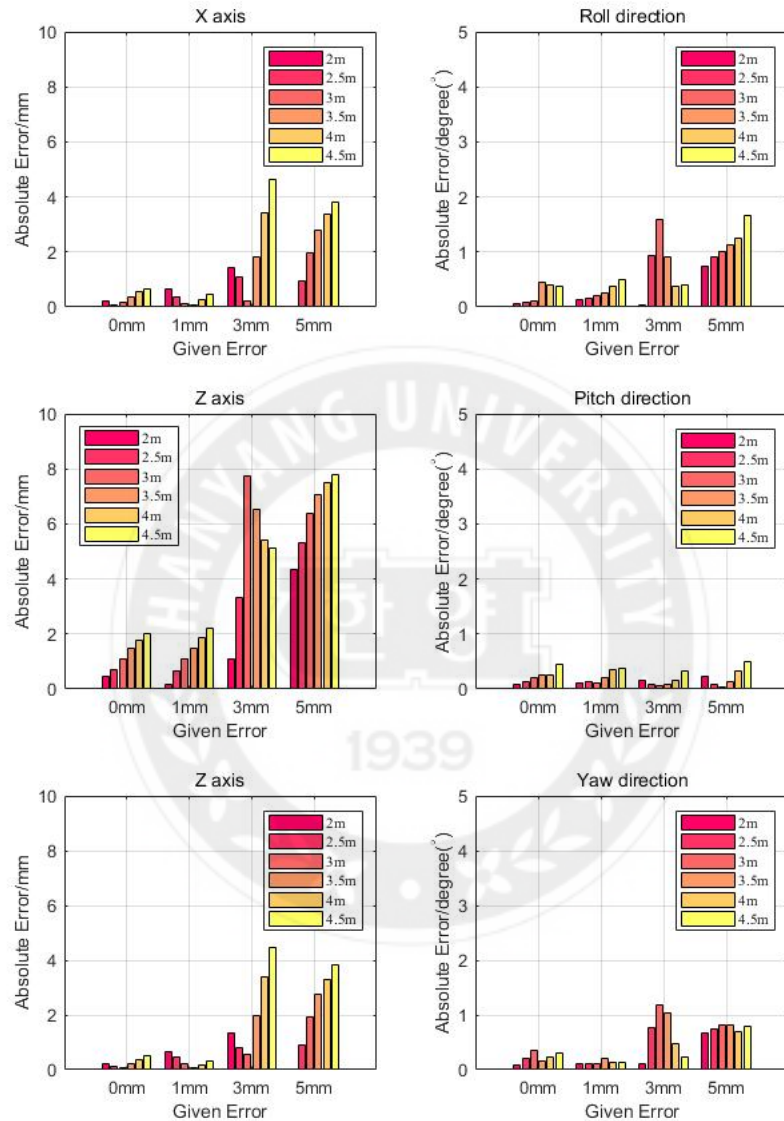


Figure 4.5: Pose accuracy according to the errors(Specific)

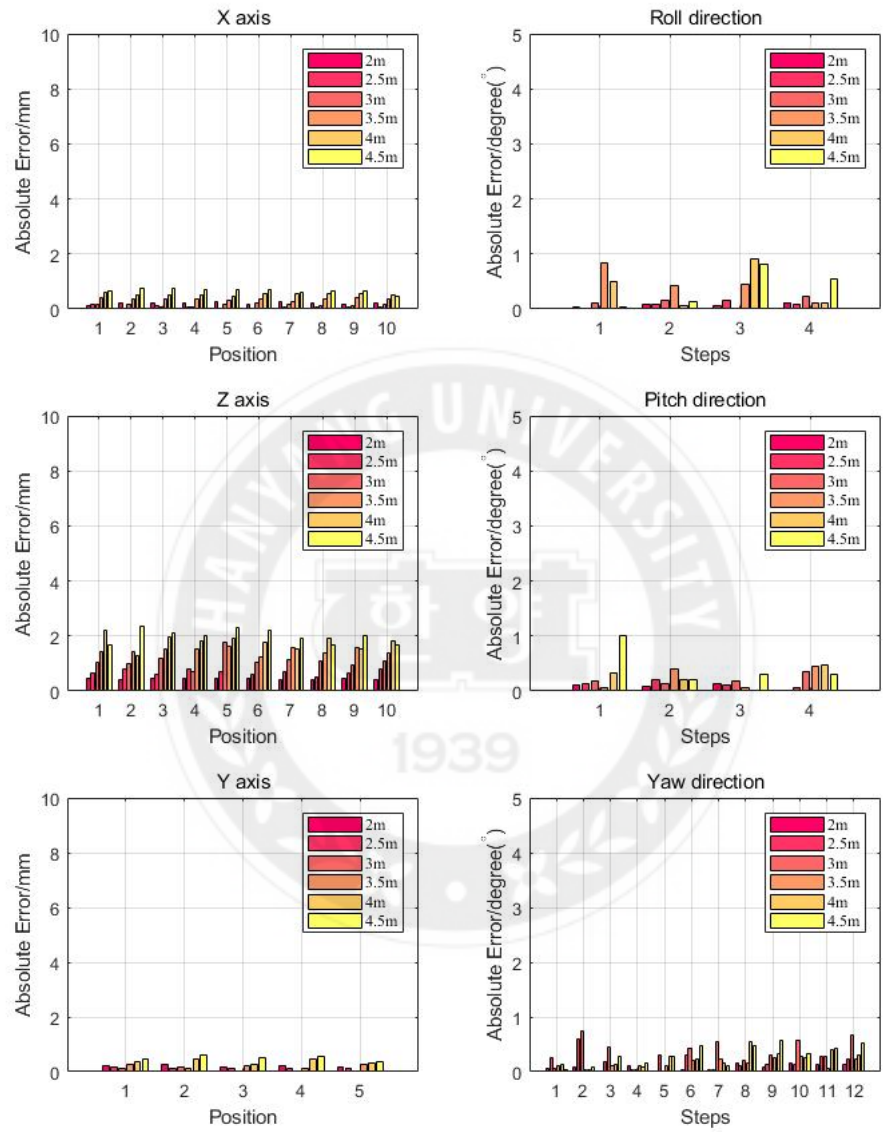


Figure 4.6: Pose accuracy given error 0mm

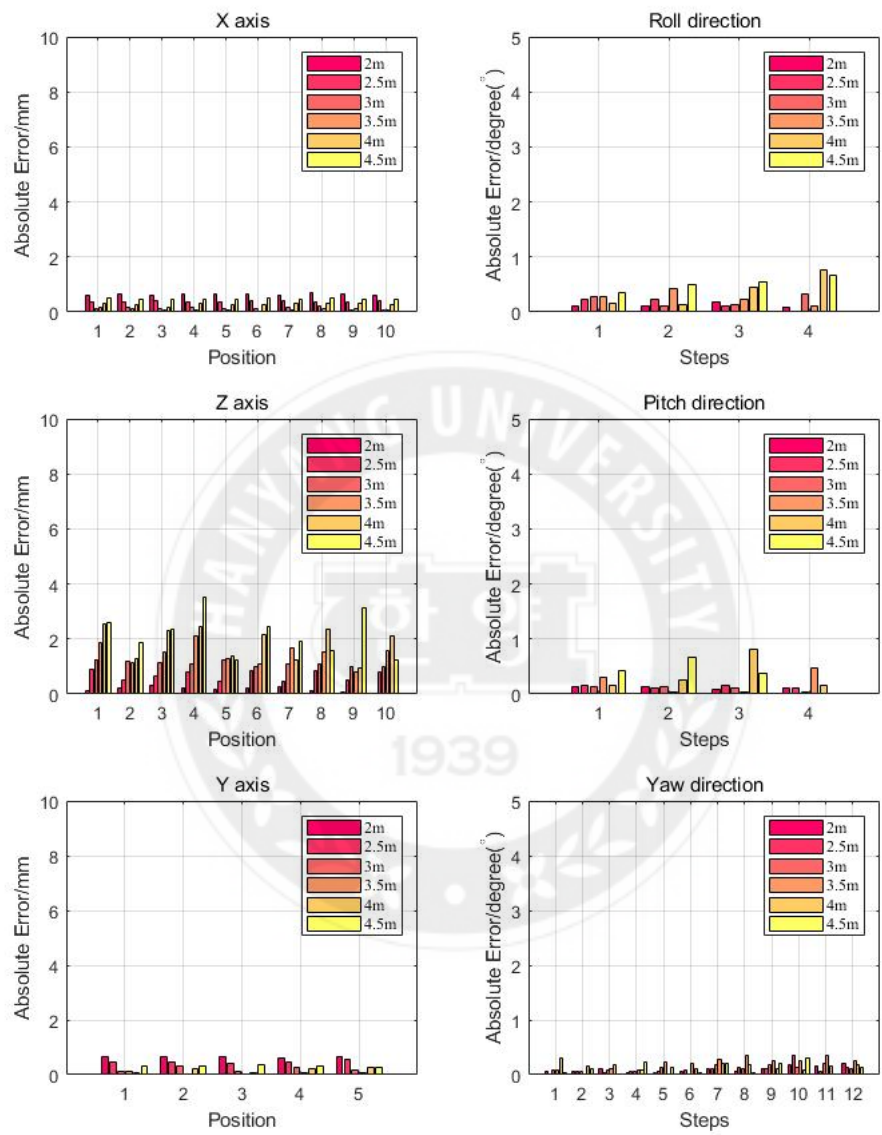


Figure 4.7: Pose accuracy given error 1mm

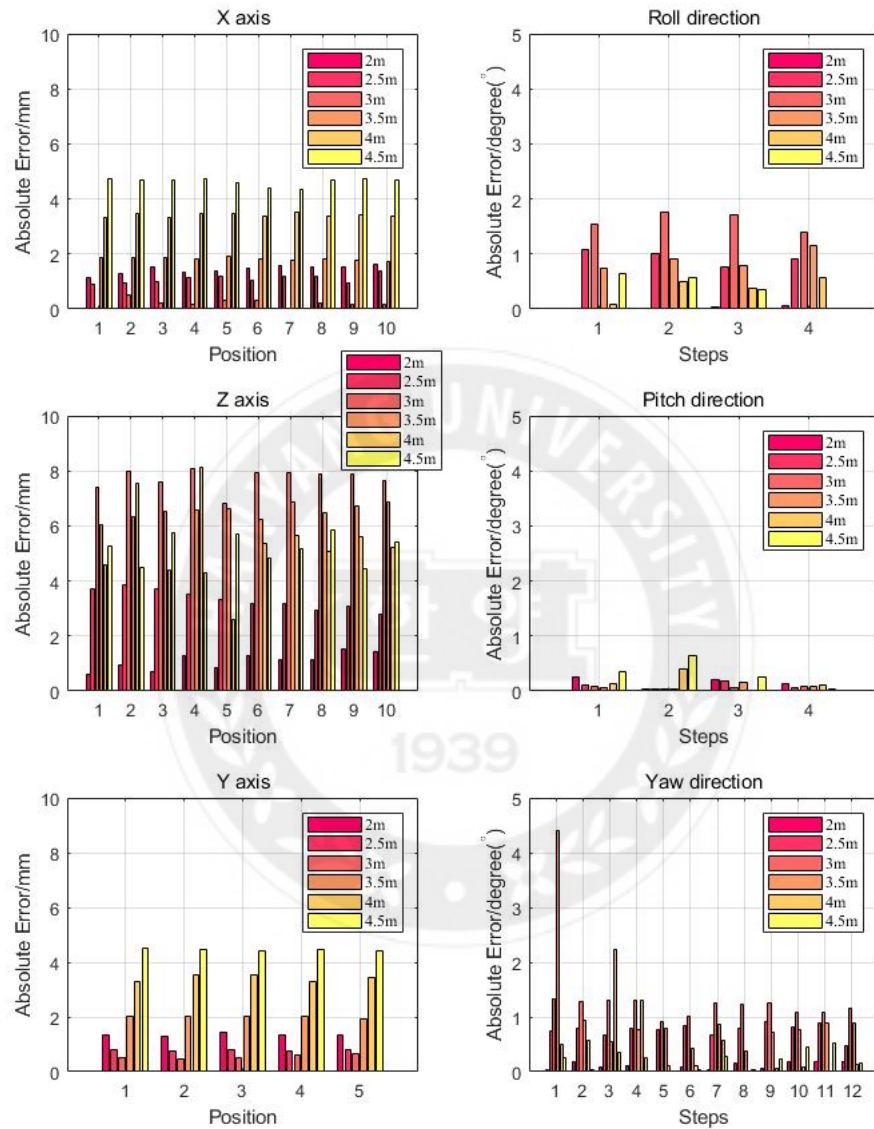


Figure 4.8: Pose accuracy given error 3mm

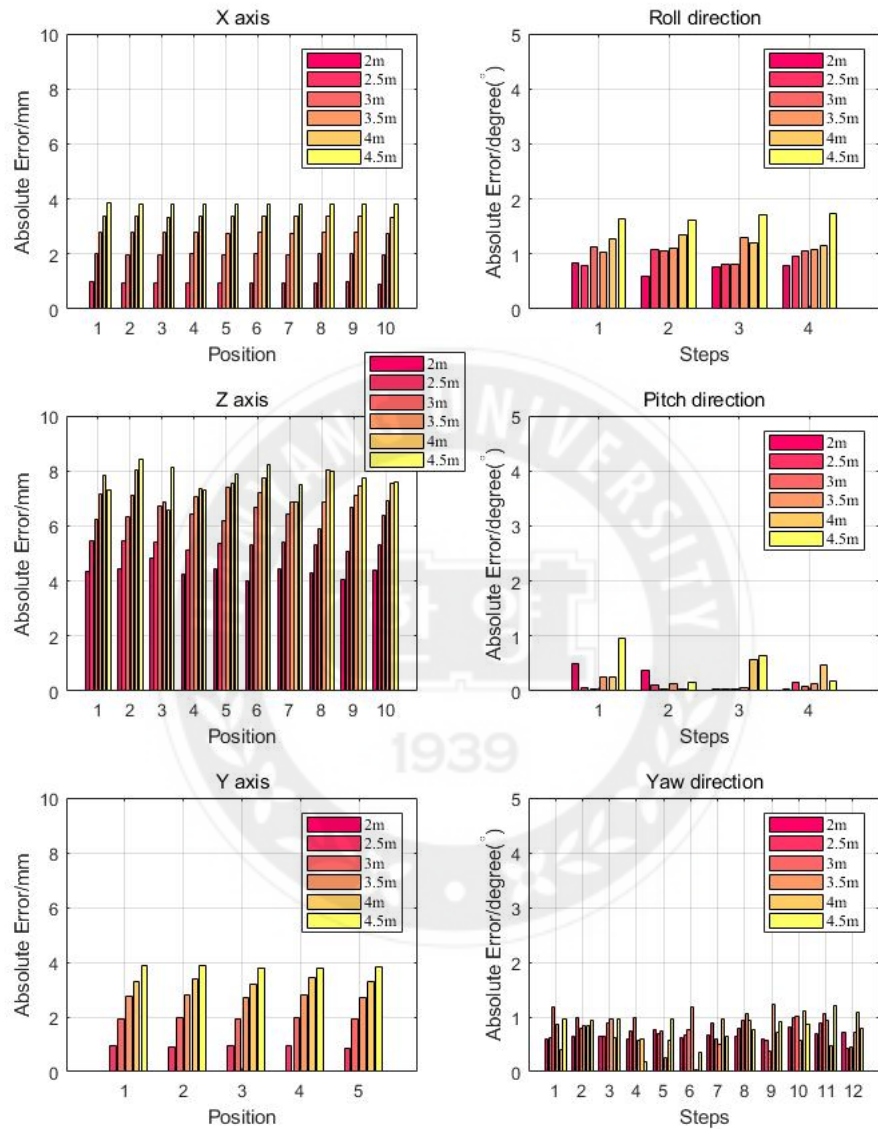


Figure 4.9: Pose accuracy given error 5mm

## 4.2 Experiment 2

Experiment 2 shows the evaluation of pose estimation accuracy with various environment set(table 4.3) in Vive system.

|        | Base station |          |            |            | Marker Height |
|--------|--------------|----------|------------|------------|---------------|
|        | Height       | Baseline | $\theta_1$ | $\theta_2$ |               |
| Case 1 | 1.7m         | 0.3m     | 0°         | 0°         | 0.95m         |
| Case 2 | 1.7m         | 0.6m     | 0°         | 0°         | 0.95m         |
| Case 3 | 1.7m         | 1m       | 5°         | 5°         | 0.95m         |
| Case 4 | 1.7m         | 1m       | 5°         | 10°        | 0.95m         |

Table 4.3: Setup experiment 2

The detecting range of base station is  $120^\circ$ . As laser planes are rotating, if an object gets off its center, estimated angles are different in the same object. It affects the results.

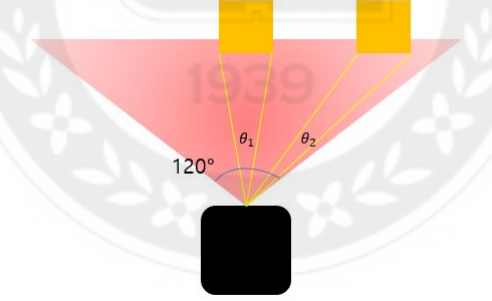


Figure 4.10: Detecting range of base station and difference between center direction and others( $\theta_1 > \theta_2$ )

Case 1 and Case 2 set the base stations angles,aligned optical axis with marker z-axis in figure (4.11). Average error of position is each  $1.1275mm$  and  $1.7511mm$ , orientation is each  $0.2028^\circ$  and  $0.3117^\circ$ . From two cases, as the object is far from its center, we can see that the error increases.

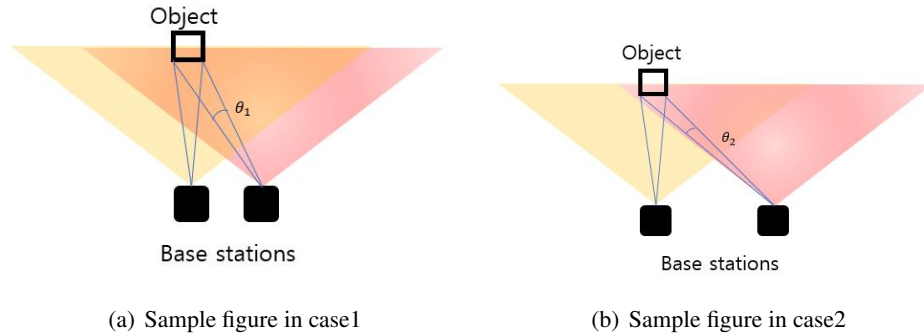


Figure 4.11: Sample figure in case1 and case2

Case 3 and Case 4 does not align the optical axis with marker z-axis, base stations look at the marker. And average errors of position and orientation are  $1.4402\text{mm}$  and  $0.2472^\circ$  in case3 and  $0.8836\text{mm}$  and  $0.3282^\circ$  in case4. Overall errors are low compared with previous cases because the optical axis of base stations is more closer to the marker.

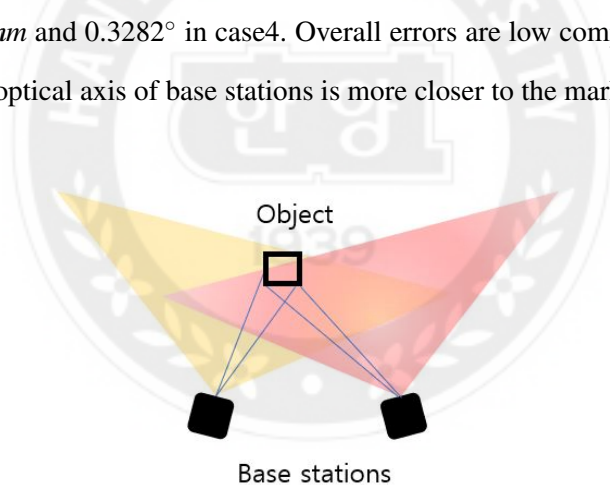


Figure 4.12: Base stations look at the marker

|         | Position [mm] |        |        |         | Orientation [°] |        |        |         |
|---------|---------------|--------|--------|---------|-----------------|--------|--------|---------|
|         | x-axis        | y-axis | z-axis | Average | roll            | pitch  | yaw    | Average |
| Case 1  | 0.6528        | 0.5647 | 2.1650 | 1.1275  | 0.2545          | 0.1050 | 0.2490 | 0.2028  |
| Case 2  | 0.9880        | 0.9688 | 3.2966 | 1.7511  | 0.4113          | 0.1906 | 0.3331 | 0.3117  |
| Case 3  | 0.7408        | 0.6911 | 2.8887 | 1.4402  | 0.2857          | 0.2233 | 0.2326 | 0.2472  |
| Case 4  | 0.4119        | 0.4344 | 1.8044 | 0.8836  | 0.4415          | 0.2283 | 0.3147 | 0.3282  |
| Average | 0.6984        | 0.6647 | 2.5387 | 1.3006  | 0.3483          | 0.1868 | 0.2823 | 0.2725  |

Table 4.4: Experiment2 result

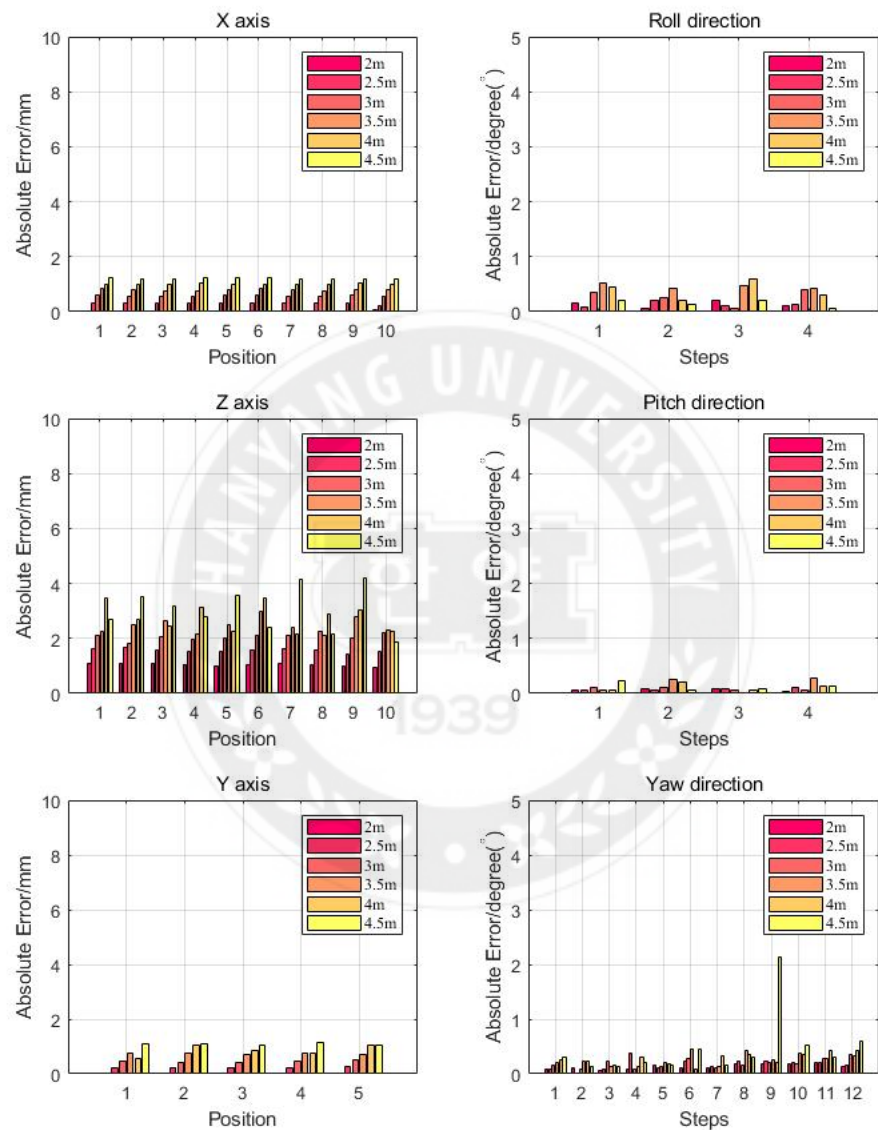


Figure 4.13: Various environment set of case 1

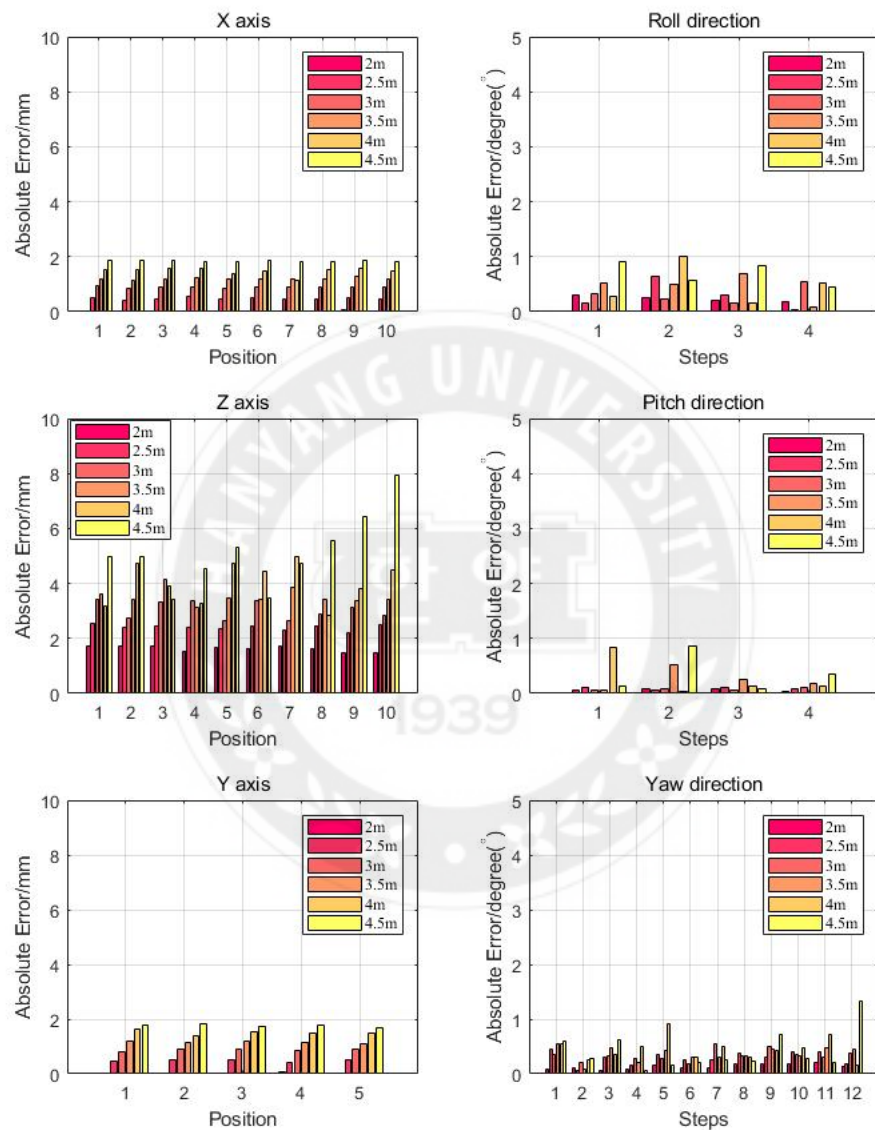


Figure 4.14: Various environment set of case 2

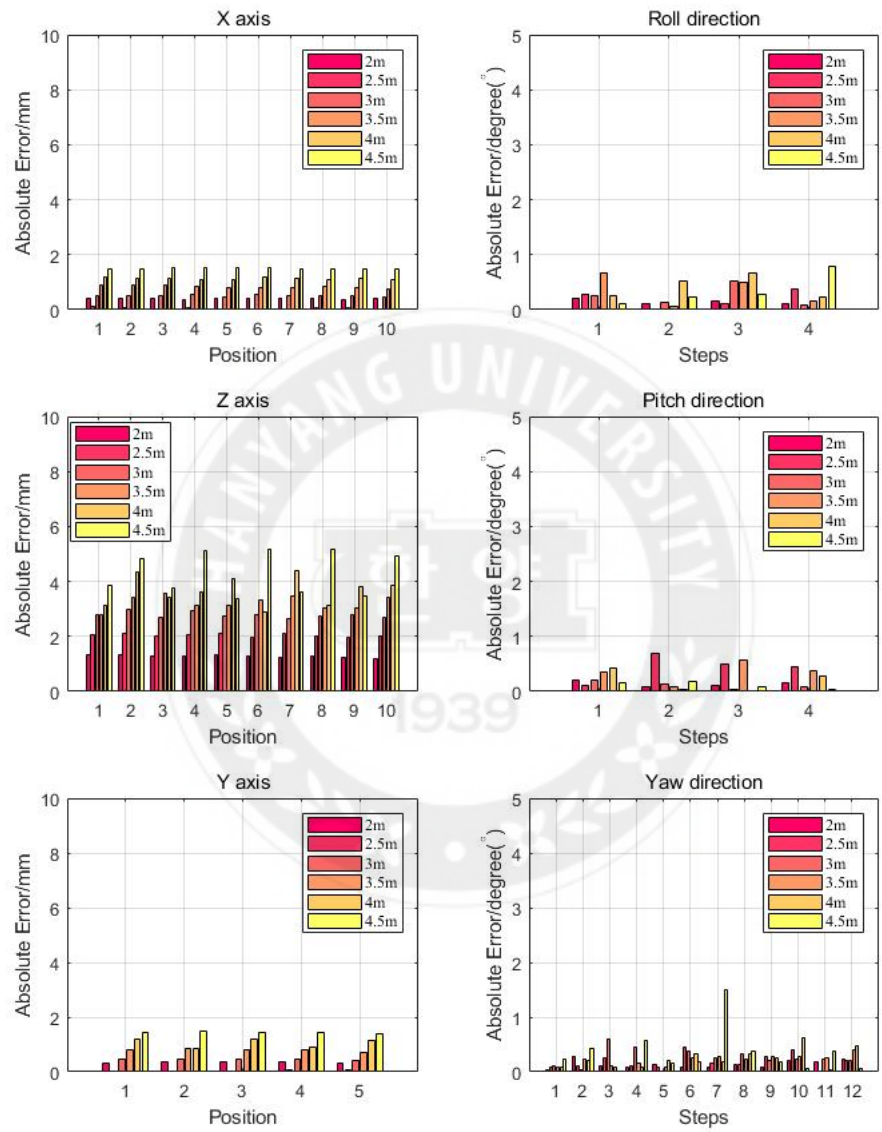


Figure 4.15: Various environment set of case 3

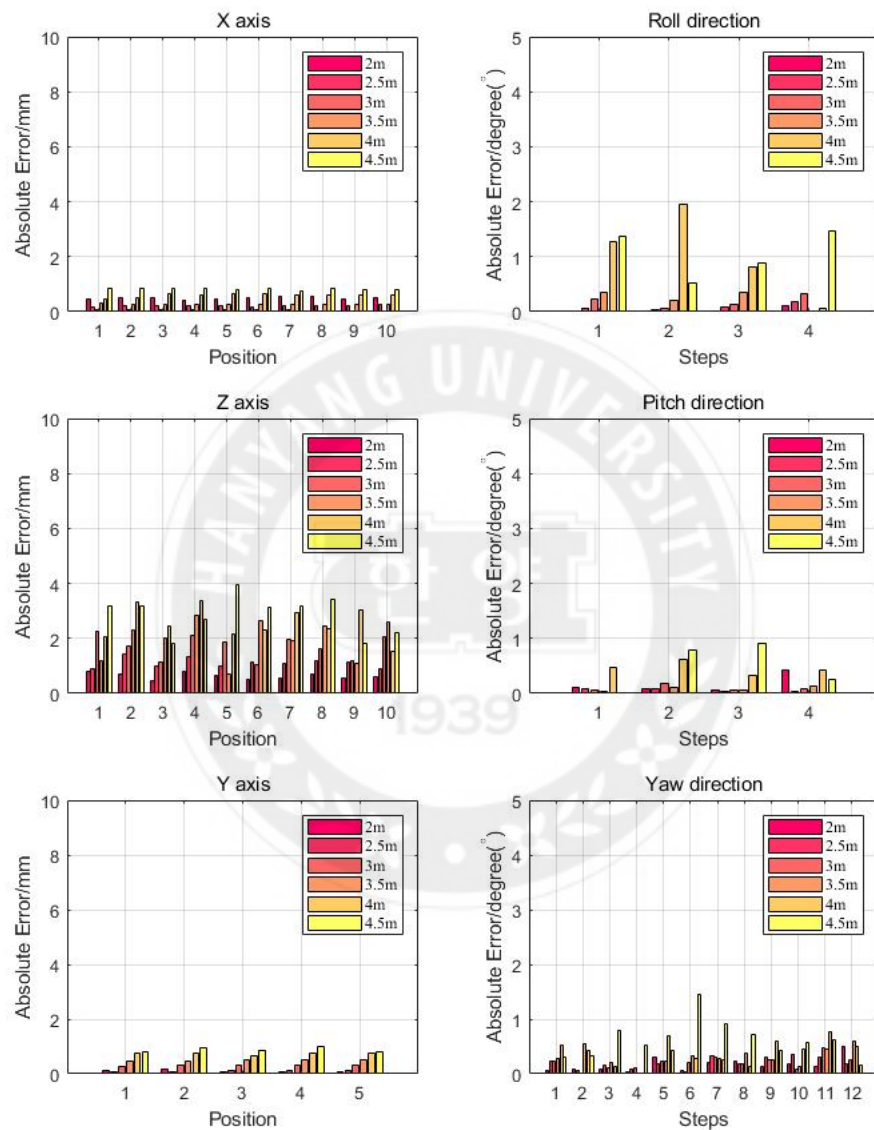


Figure 4.16: Various environment set of case 4

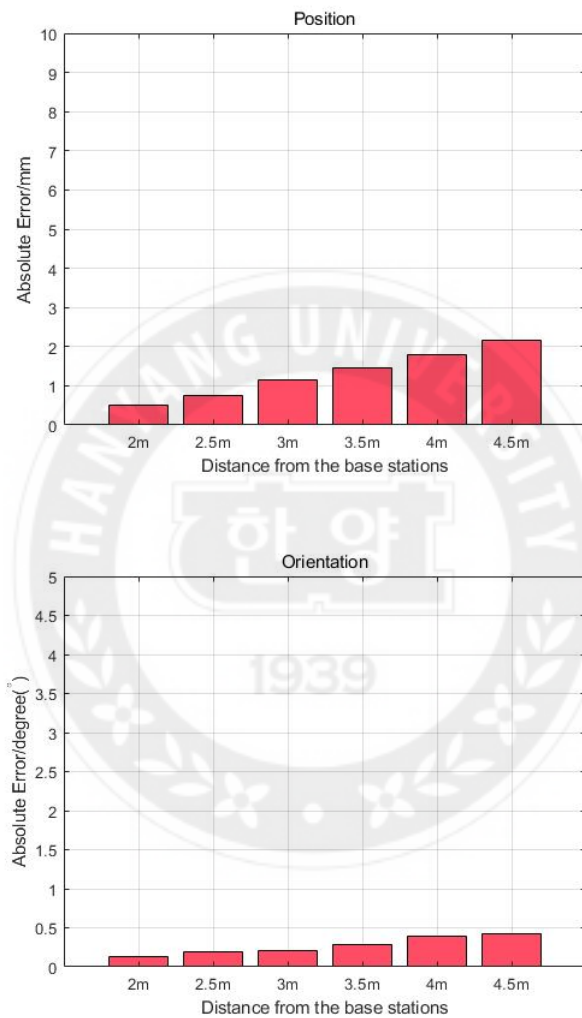
**Average pose accuracy**

Figure 4.17: Average pose accuracy above four data

### 4.3 Experiment 3

Experiment 3 is evaluation of pose accuracy compared with the commercial system (NDI) which has 0.33mm RMS(Root mean square) in the same conditions. A system overview is presented in the figure (4.18).

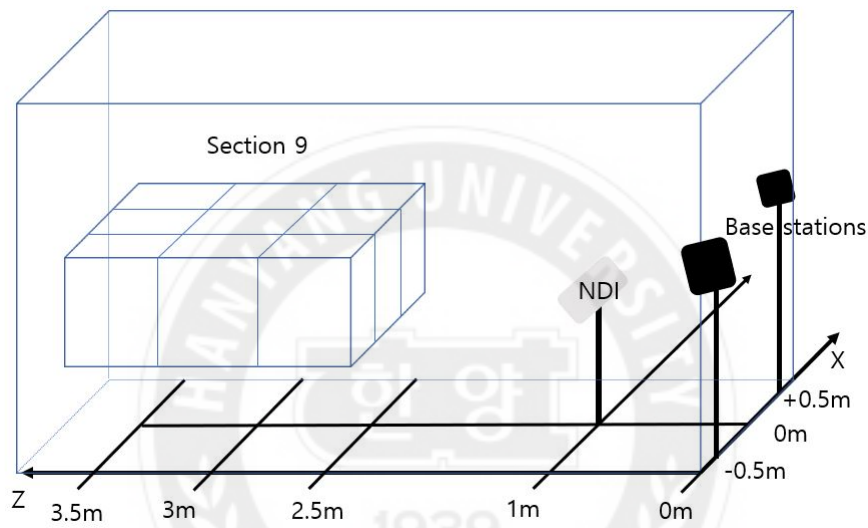


Figure 4.18: System in experiment3

To detect marker, NDI system and Vive system need at least each 1m and 2m away. And the overlap areas where can be detected in Vive and NDI system were divided into nine sections. Environment set is shown in table (4.5).

| Base station set |          |            |            | Marker |
|------------------|----------|------------|------------|--------|
| Height           | Baseline | $\theta_1$ | $\theta_2$ | Height |
| 2m               | 1m       | 10°        | 20°        | 1.3m   |

Table 4.5: Setup experiment3

Average errors of pose are  $0.7444\text{mm}$  and  $0.1885^\circ$  in Vive system and  $0.0404\text{mm}$  and  $0.0858^\circ$  in NDI system. As we can see the results, NDI system is stable and accuracy is high in its detected all areas and Vive system is unstable and accuracy is low relative to NDI. But accuracy of Vive system is less than  $1\text{mm}$ , it is appropriate to use. A merits of Vive system is that detecting range is wide than NDI system and cost is much lower and robustness in light.

Another characteristic in Vive system is that the accuracy of z-axis is weakness compared with its x and y-axis. As rotating pitch direction is less involved z-axis components, it has similar performance as NDI in pitch direction.

|      | Position [mm] |        |        |         | Orientation [°] |        |        |         |
|------|---------------|--------|--------|---------|-----------------|--------|--------|---------|
|      | x-axis        | y-axis | z-axis | Average | roll            | pitch  | yaw    | Average |
| Vive | 0.2782        | 0.2978 | 1.6572 | 0.7444  | 0.2665          | 0.0942 | 0.2048 | 0.1885  |
| NDI  | 0.0395        | 0.0164 | 0.0652 | 0.0404  | 0.0877          | 0.0959 | 0.0738 | 0.0858  |

Table 4.6: Experiment3 result

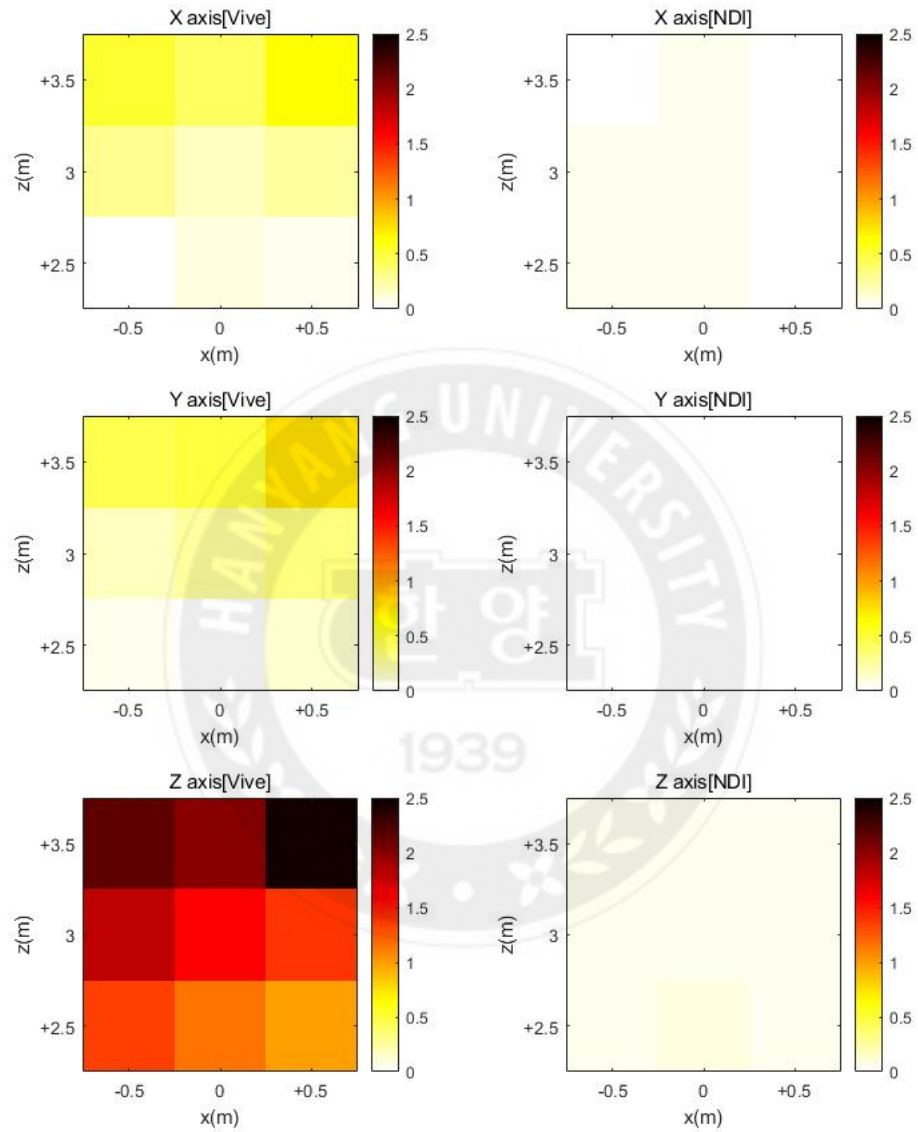


Figure 4.19: Position accuracy with NDI system

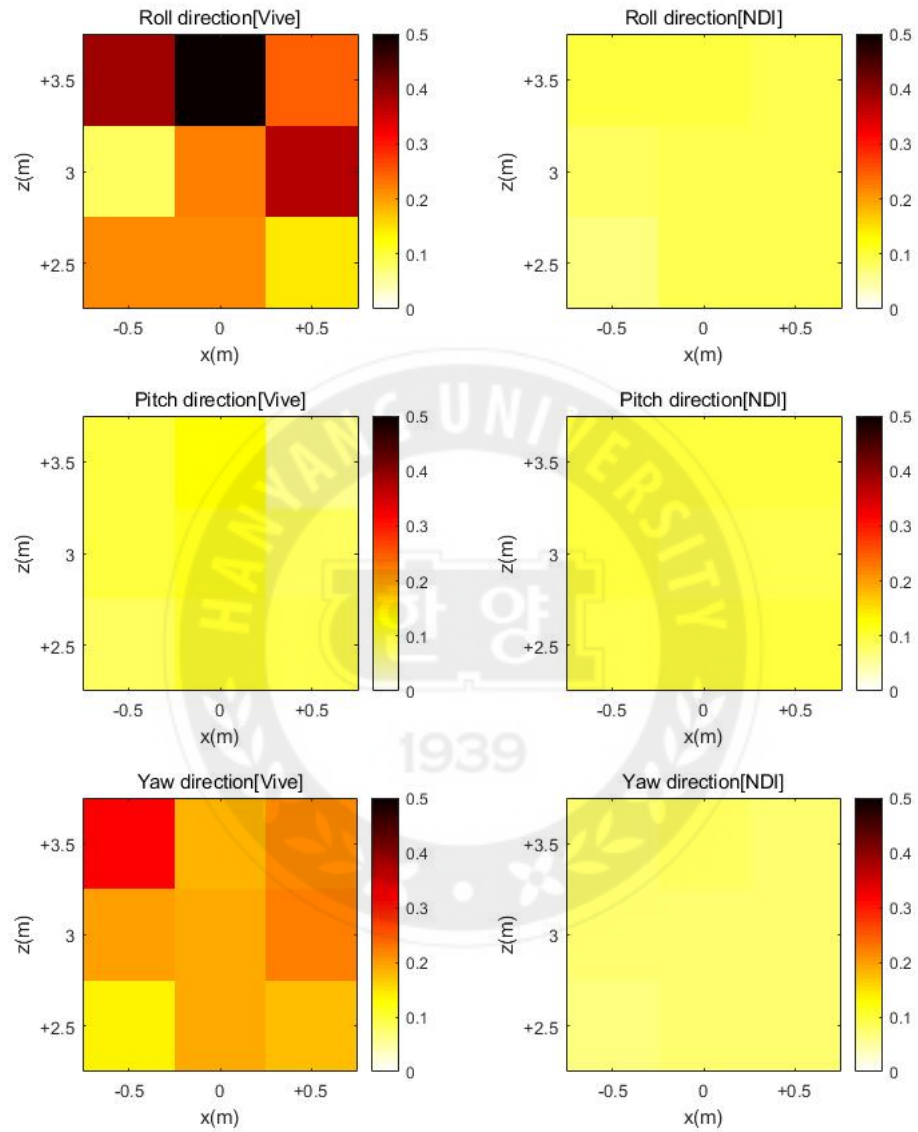


Figure 4.20: Orientation accuracy with NDI system

# Chapter 5

## CONCLUDING REMARKS

In this thesis, a new method of calibration has been proposed and evaluated a pose estimation precision with the designed marker in the Vive system. It also contains the procedure of pose estimation using two lighthouses with the designed marker. The Vive is a type of indoor positioning system that is not only low cost but also high precision.

Calibration is necessary to estimate the accurate pose of the two coordinate systems. However, a requirement of the calibration is difficult to measure the exact distance among the location of the all sensors attached to the designed marker due to manufacturing faults in marker and attached sensors.

The proposed method has only one linear stage and used one sensor. Although the developed method is spending more time as compared to the existing methods, it is robust to errors. From the experiment results, it is revealed that the precision of calibration allows error of 1 mm. Additionally, the evaluation of system precision has been shown by experiments.

The result of experiment 1 shows the pose precision according to the calibration precision, given the error 1mm, 3mm and 5mm. The large error was given, The more accuracy

error increases. Especially, a  $5mm$  error can be seen as an increase of about six times in position and three times in orientation over a non-error. The result of experiment 2 shows the pose estimation precision of the designed marker in Vive system. Average error of position is  $1.3006mm$  and orientation is  $0.2725^\circ$ . The result of experiment 3 show the evaluation of pose estimation accuracy compare with NDI system which has  $0.33mm$  RMS accuracy. The average precision of position is  $0.0404mm$  and  $0.7444mm$  and orientation is  $0.0858^\circ$  and  $0.1885^\circ$  in each NDI and Vive system.

The performance of Vive system is not uniform and it alters on the environmental setup of the lighthouse. Unlike Vive system, the performance of NDI system is constant, but it is very sensitive to light. The detecting area of Vive system is wider than NDI system. The Vive system detection area has a range of 2m to 4.5m from the lighthouses location. While the detection area range of NDI system is about 2m.

The limitation of this system is relatively unstable, it depends on the environmental setup and minor vibration of lighthouse. Manual estimation of orientation in the experiment may also another cause of errors.

## BIBLIOGRAPHY

- [1] Chessboard, “7x9 chessboard.” [https://www.mrpt.org/downloads/camera-calibration-checker-board\\_9x7.pdf](https://www.mrpt.org/downloads/camera-calibration-checker-board_9x7.pdf), accessed 02 July 2018.
- [2] Wiki, “Indoor Positioning System.” [https://en.wikipedia.org/wiki/Indoor\\_positioning\\_system](https://en.wikipedia.org/wiki/Indoor_positioning_system), accessed 21 Jun 2018.
- [3] Wiki, “HTC VIVE.” [https://en.wikipedia.org/wiki/HTC\\_Vive](https://en.wikipedia.org/wiki/HTC_Vive), accessed 05 Jun 2018.
- [4] Vive, “VIVE.” <https://www.vive.com/us/>, accessed 02 Jun 2018.
- [5] NDI, “NDI Measurement.” <https://www.ndigital.com/medical/products/polaris-family>, accessed 02 Oct 2018.
- [6] E. Cuervo, “Beyond reality: Head-mounted displays for mobile systems researchers,” *GetMobile: Mobile Computing and Communications*, vol. 21, no. 2, pp. 9–15, 2017.
- [7] D. C. Niehorster, L. Li, and M. Lappe, “The accuracy and precision of position and orientation tracking in the htc vive virtual reality system for scientific research,” *i-Perception*, vol. 8, no. 3, p. 2041669517708205, 2017.

- [8] M. Maciejewski, M. Piszczeck, and M. Pomianek, “Testing the steamvr trackers operation correctness with the optitrack system,” in *Thirteenth Integrated Optics: Sensors, Sensing Structures and Methods Conference*, vol. 10830, p. 10, SPIE.
- [9] D. R. Quiñones, G. Lopes, D. Kim, C. Honnet, D. Moratal, and A. Kampff, “Hive tracker: a tiny, low-cost, and scalable device for sub-millimetric 3d positioning,” *Augmented Human*, vol. 9, 2018.
- [10] Wiki, “Perspective n-points.” <https://en.wikipedia.org/wiki/Perspective-n-Point>, accessed 01 March 2018.
- [11] J. A. Hesch and S. I. Roumeliotis, “A direct least-squares (dls) method for pnp,” in *Computer Vision (ICCV), 2011 IEEE International Conference on*, pp. 383–390, IEEE.
- [12] B. K. P. Horn, “Closed-form solution of absolute orientation using unit quaternions,” *Journal of the Optical Society of America a-Optics Image Science and Vision*, vol. 4, no. 4, pp. 629–642, 1987.
- [13] L. Quan and Z. Lan, “Linear n-point camera pose determination,” *IEEE Transactions on pattern analysis and machine intelligence*, vol. 21, no. 8, pp. 774–780, 1999.
- [14] P. David, D. Dementhon, R. Duraiswami, and H. Samet, “Softposit: Simultaneous pose and correspondence determination,” *International Journal of Computer Vision*, vol. 59, no. 3, pp. 259–284, 2004.
- [15] M. A. Fischler and R. C. Bolles, *Random sample consensus: a paradigm for model fitting with applications to image analysis and automated cartography*, pp. 726–740. Elsevier, 1987.

- [16] X.-S. Gao, X.-R. Hou, J. Tang, and H.-F. Cheng, “Complete solution classification for the perspective-three-point problem,” *IEEE transactions on pattern analysis and machine intelligence*, vol. 25, no. 8, pp. 930–943, 2003.
- [17] X.-S. Gao and J. Tang, “On the number of solutions for the p4p problem,” *MM Research Preprints*, vol. 21, pp. 64–76, 2002.
- [18] R. Horaud, B. Conio, O. Leboulleux, and B. Lacolle, “An analytic solution for the perspective 4-point problem,” in *Computer Vision and Pattern Recognition, 1989. Proceedings CVPR'89., IEEE Computer Society Conference on*, pp. 500–507, IEEE.
- [19] Z. Hu and F. Wu, “A note on the number of solutions of the noncoplanar p4p problem,” *IEEE Transactions on Pattern Analysis and Machine Intelligence*, vol. 24, no. 4, pp. 550–555, 2002.
- [20] Y. Yang, D. Weng, D. Li, and H. Xun, “An improved method of pose estimation for lighthouse base station extension,” *Sensors*, vol. 17, no. 10, p. 2411, 2017.
- [21] S. Islam, B. Ionescu, C. Gadea, and D. Ionescu, “Indoor positional tracking using dual-axis rotating laser sweeps,” in *Instrumentation and Measurement Technology Conference Proceedings (I2MTC), 2016 IEEE International*, pp. 1–6, IEEE.
- [22] Wiki, “Base Stations.” [https://xinreality.com/wiki/Base\\_Stations](https://xinreality.com/wiki/Base_Stations), accessed 16 April 2018.
- [23] Z. Zhang, “A flexible new technique for camera calibration,” *IEEE Transactions on pattern analysis and machine intelligence*, vol. 22, 2000.
- [24] J. Heikkila and O. Silven, “A four-step camera calibration procedure with implicit

- image correction,” in *Computer Vision and Pattern Recognition, 1997. Proceedings., 1997 IEEE Computer Society Conference on*, pp. 1106–1112, IEEE, 1997.
- [25] A. Shtuchkin, “DIY Position Tracking using HTC Vive’s Lighthouse.” <https://github.com/ashtuchkin/vive-diy-position-sensor> , accessed 05 Jun 2018.
- [26] T. Hudson, “HTC Vive Lighthouse.” [https://trmm.net/Lighthouse#HTC\\_Vive\\_Lighthouse](https://trmm.net/Lighthouse#HTC_Vive_Lighthouse) , accessed 05 Jun 2018.
- [27] J. J. Craig, *Introduction to robotics: mechanics and control*, vol. 3. Pearson/Prentice Hall Upper Saddle River, NJ, USA:, 2005.
- [28] D. H. Eberly, *3D game engine design: a practical approach to real-time computer graphics*. CRC Press, 2006.
- [29] A. Mathai and R. Katiyar, “A new algorithm for nonlinear least squares,” vol. 81, 08 1996.

## 국문 요지

2015년, 가상현실 시스템인 Vive는 HTC와 Valve사에서 개발됐다. 이 시스템은 실내 위치 측정 시스템(Indoor Positioning System, 이하 IPS)의 한 종류이며 적외선 레이저를 기반으로 한다. 물체의 포즈(위치와 자세)를 측정하는데 있어서 "라이트 하우스" 또는 "베이스 스테이션"이라는 장비를 사용하는데, 기존에 사용되고 있는 IPS에 비해 가격이 저렴하고 높은 정확성과 낮은 자연성을 가지고 있어 많은 주목을 받고 있다.

하나의 카메라로 물체(Rigid body)의 포즈추정을 할 때, 물체의 기하학적 특징점이 최소 3개가 필요하다. 그 점으로부터 PnP(Perspective n-points) 방법을 사용하여 카메라 좌표계에 대한 물체의 포즈를 추정할 수 있다. 두 개의 라이트 하우스로 카메라 시스템의 스테레오 비전처럼 삼각법(Triangulation)을 사용하여 물체의 포즈를 추정할 수 있다. 삼각법을 사용하기 위해서는 두 라이트 하우스 간의 위치와 회전관계를 알아야한다. 이러한 관계를 찾는 것을 캘리브레이션이라고 한다. 캘리브레이션 할 때, 이미 알고 있는 물체의 기하학적 정보(예, 특징점들 간 상대적 거리정보)를 사용한다. 이 정보에 오차가 있으면 정확한 캘리브레이션이 되지 않고, 물체의 포즈를 추정할 때 오차가 발생한다. Vive 시스템에서 캘리브레이션을 하려면 특징점이 있는 물체가 필요하고 특징점들 간의 정확한 기하학적 정보가 필요하다. 여기서 특징점은 라이트 하우스에서 나오는 적외선 레이저를 감지하는 센서이다. 이러한 센서를 부착하여 캘리브레이션과 포즈추정을 위해 직접 물체를 제작하여 사용하는데, 이렇게 제작된 물체를 마커라고 한다. 하지만 마커를 제작하면서 발생되는 가공오차와 제작된 마커에 센서를 부착하면서 발생하는 오차로 인해 마커에 위치한 센서들간의 정확한 기하학적 정보를 얻는데 어려움이 있다.

본 논문에서는 Vive 시스템 사용을 위한 캘리브레이션 과정에서 센서 간의 정확한 기하학 정보를 얻을 수 있는 새로운 캘리브레이션 방법을 제안한다. 실험을 통하여 센서의

기하학적 정보 오차에 따른 포즈 추정 정확성을 검증한다. 또한, 본 논문에서 제안하는 방법을 적용하여 마커의 포즈 정확성을 검증하고 상용 시스템과 포즈 정확성을 비교와 분석을 해본다. 실험 결과로는 캘리브레이션 과정에서 5mm의 기하학적 오차가 발생하면 오차가 발생하지 않을 때보다 위치는 약 6배, 자세는 약 3배 정도 정확성이 떨어진다. 상용 시스템은 물체의 포즈를 매우 정확하게 추정하지만 자연 광에 민감하여 오류가 발생할 수 있으며 감지되는 영역이 약  $3m^3$ 로 한정적이다. 반면에 라이트 하우스 시스템은 상용 시스템보다 상대적으로 광 축 방향에 대한 정확성이 떨어지지만 자연 광에 의한 오류가 없고 감지되는 영역이 약  $10m^3$ 으로 3배이상 크다. 그리고 100배 이상 저렴하기 때문에 가격 경쟁력을 가지고 있다. 결론적으로 위치오차가 1.5mm이상, 자세오차가  $0.3^\circ$  이상 허용되는 포즈추정 어플리케이션에서는 Vive 시스템을 저렴하고 높은 정확성을 가진 IPS로 적용 가능하다.



# Declaration of Ethical Conduct in Research

I, as a graduate student of Hanyang University, hereby declare that I have abided by the following Code of Research Ethics while writing this dissertation thesis, during my degree program.

"First, I have strived to be honest in my conduct, to produce valid and reliable research conforming with the guidance of my thesis supervisor, and I affirm that my thesis contains honest, fair and reasonable conclusions based on my own careful research under the guidance of my thesis supervisor.

Second, I have not committed any acts that may discredit or damage the credibility of my research. These include, but are not limited to : falsification, distortion of research findings or plagiarism.

Third, I need to go through with Copykiller Program(Internet-based Plagiarism-prevention service) before submitting a thesis."

DECEMBER 12, 2018

Degree : Master

Department : DEPARTMENT OF ELECTRICAL AND ELECTRONIC ENGINEERING

Thesis Supervisor : Lee, Sungon

Name : KIM DONG YEON

*Dongyeon*  
Signature

## 연구 윤리 서약서

본인은 한양대학교 대학원생으로서 이 학위논문 작성 과정에서 다음과 같이 연구 윤리의 기본 원칙을 준수하였음을 서약합니다.

첫째, 지도교수의 지도를 받아 정직하고 엄정한 연구를 수행하여 학위논문을 작성한다.

둘째, 논문 작성시 위조, 변조, 표절 등 학문적 진실성을 훼손하는 어떤 연구 부정행위도 하지 않는다.

셋째, 논문 작성시 논문유사도 검증시스템 "카피킬러" 등을 거쳐야 한다.

2018년12월12일

학위명 : 석사

학과 : 전자공학과

지도교수 : 이성온

성명 : 김동연

*DongYeon Kim*

한 양 대 학 교 대 학 원 장 귀 하